every step should be 500 mm, after being multiplied by the corrective coefficient obtained earlier, this value is shown in Figure. 4.15d. Finally, speed is obtained from the product of the estimated amplitude and the cadence, in Figure. 4.15e.

Moreover, tests in which the pace of the gait is changed during the experiments have been done. The cadence is changed from 1 step/sec to 0,5 step/sec and it is shown that the estimated cadence changes as desired, as observable in Figure.4.16c.

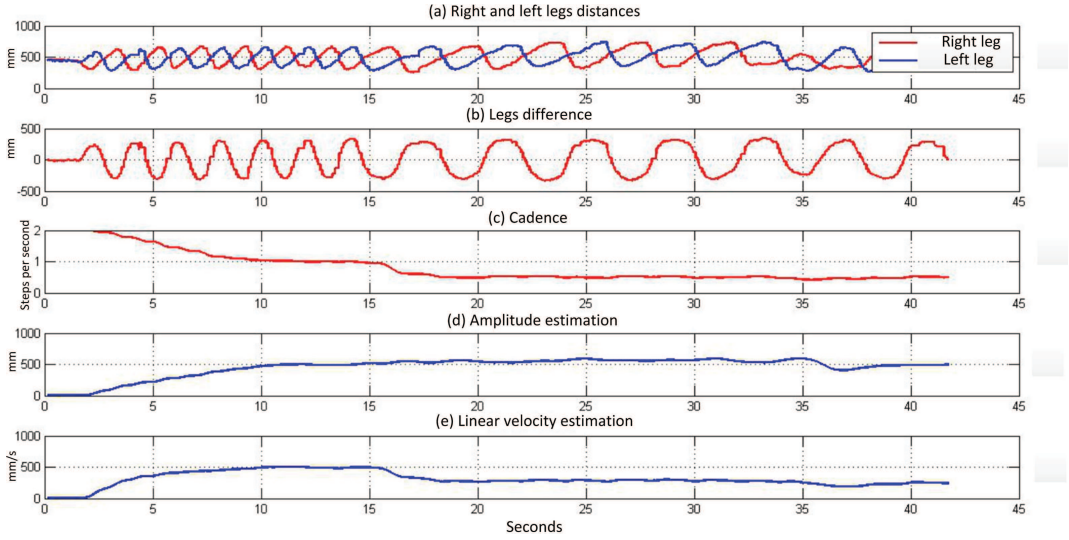

FIGURE 4.16: Results of test done with 1 step/sec walking speed for the first section, approximately 15 seconds, and with 0.5 step/sec for the following 25 seconds.(a) Distance from the LRF of the legs, the right one in red and the left one in blue, (b) Difference in between the position of the two legs, (c) cadence estimated by the algorithm WFLC (d) Amplitude estimated by the algorithm FLC (with the CC); (e) speed of the amplitude of the product obtained by the cadence estimated.

As can be seen in Figure. 4.17(a) and Figure. 4.18(a), the amplitude error is almost constant for different user's speeds and groups of users divided by size, this is mainly due to the fact that tape marks the ground at every step. Taller people have a higher percentage of error in getting a good cadence and speed, while people of small and medium size have very similar error, as visible in Figure. 4.17(a) and Figure. 4.17(b). This could be due to the chosen step length proposed for the experiments, which is 500 mm and is probably not long enough for a tall person to walk comfortably.

Furthermore, it is observed in Figure. 4.18(a) and Figure. 4.18(b), that when performing the low-speed walking test one is more likely to make a larger error in percentage for cadence and speed estimation. This can be caused by the too low imposed speed (250 mm/s). Note that users without locomotion-related pathologies are not used to walk at such a low speed.

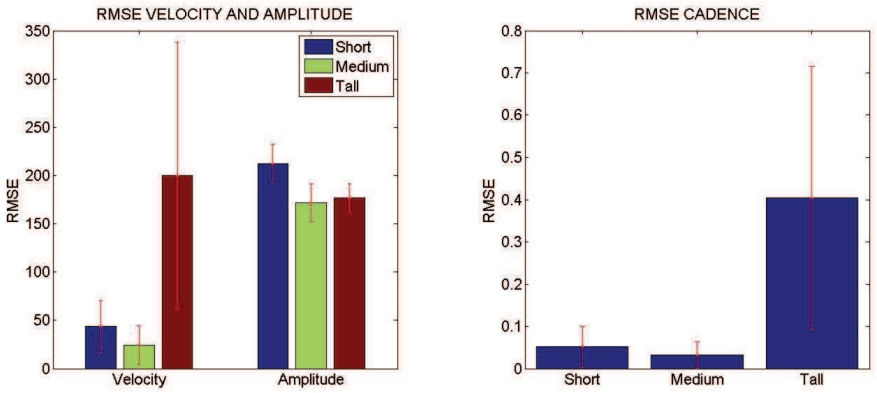

(a) (b)

FIGURE 4.17: (A) Mean square error of velocity and amplitude tested by dividing users into three categories on the basis of their height, in blue, green and red, respectively, users short, medium and tall. (B) Mean square error of cadence of the three groups of users, short , medium and tall. The red lines are the standard deviations.

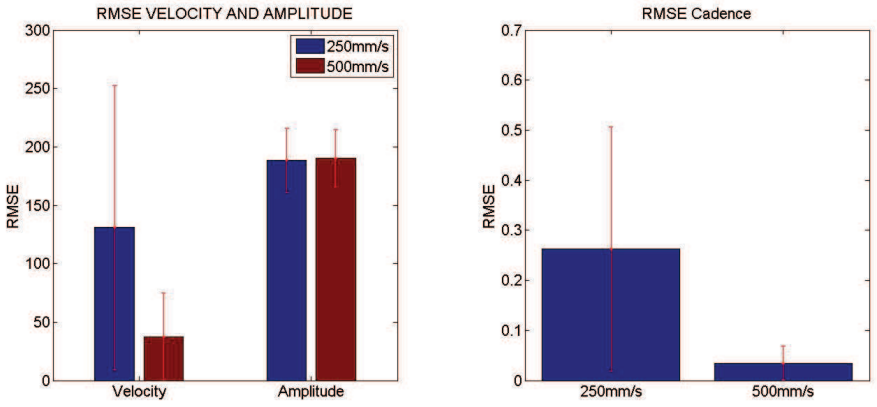

(a) (b)

FIGURE 4.18: (A) Mean square error for velocity and amplitude dividing the tests into two categories on the basis of the desired speed, blue and red, respectively, the tests performed with 250 mm / s and 500 mm / s. (B) Mean square error of cadence for the two groups of tests with different speeds. The red lines are the standard deviations.

It is noteworthy that the measured errors are not only due to approximation of the proposed algorithm, but also inaccuracies in the realization of walking gait to the indicated cadence, done with the use of a metronome and positioning errors of the feet on the ground marks.

4.3.4 Conclusions

Summing up the presented work, it is obtained a system able to detect human's intentions, as a matter of walking direction and speed and actuate the walker to provide a stable support in a comfortable position for the user. In Figure. 4.19 it's presented the general scheme of how the system works.

This control strategy is an innovation compared to [61] because it has been developed considering the parameters of the walker as continuous signals and not averaged at every gait cycle, moreover, it is completed with an innovative adaptive method to estimate the linear velocity. These modifications made the control more natural and able to respond to user's attitude variations during the step.

In blue are characterized the data coming from the user, in this case the IMU placed on the human pelvis, from which are used two parameters: the human angular velocity ω_h and the human orientation ψ_h . These two parameter come directly from the gyroscope of the IMU, which outputs the angular velocity directly and through the extraction algorithm, explained in paragraph 4.2.2, the Yaw angle.

In red are presented data from the walker, the on-board IMU from which we extract just the robot orientation ψ_r and angular velocity ω_r and the LRF-based legs detection algorithm from which we exploit the human relative orientation θ and distance d as explained in paragraph 4.2.1.

In green the detected parameters are presented, the ϕ angle obtained with eq. 4.8 and the human linear velocity obtained with the adaptive algorithms, explained in paragraph 4.3.2.

These parameters are input of the control strategy, in black, and generate the desired linear and angular speed, as explained in equations 4.3 and 4.4. Finally by means of the low level PID control, in orange, are obtained the input commands to the Right and Left motors, ω_R and ω_L.

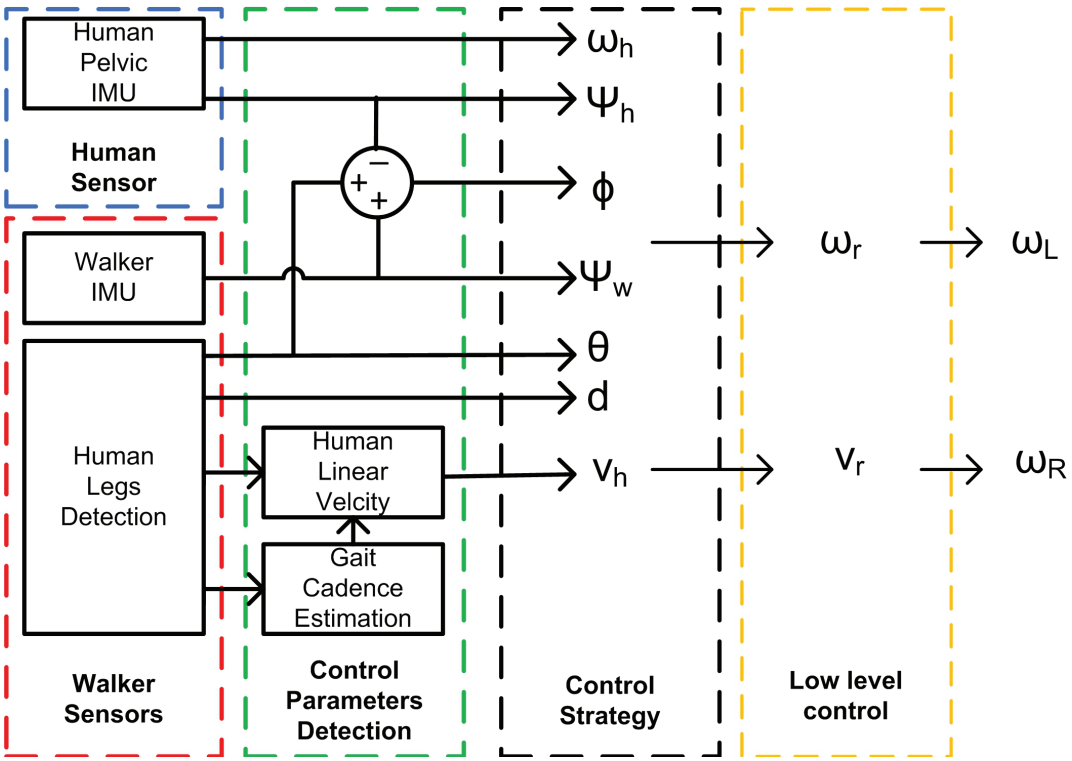

FIGURE 4.19: Scheme of the multimodal fusion of sensors on human: IMU and on Walker: IMU and LRF.
From sensors to actuators.

Chapter 5

Control Strategy based on IMU and LRF on inclined ground

The main objective of this research is to develop a control strategy that makes the assisted gait on slope as natural as possible, taking into account the optimization of user's comfort and safety. Indeed, the target is to modify the control strategy when the human-robot system runs on slopes.

In order to make the UFES smart walker able to face inclinations we have taken into account the ideas developed by other researchers in previous works, as shown in the relative State of the Art in chapter 3.

The goal pursued was to obtain an innovative compensation strategy with respect to the ones already introduced in chapter 3, not focusing on the control strategy but on the analysis of human-robot interaction on slope. The strategy has its base on the definition of a complete analysis of the kinematic interaction of human and robot on slope, so to make the control better apply to the actual physics of the problem.

Finally, the novel model of human-walker interaction on slopes was integrated into the conventional closed control loop as a supervisor block. This block modifies the control targets, depending on inclinations, in order to provide an adaptable human-walker desired relative position improving comfort and safety and enhancing user's confidence in the walker.

5.1 PIVOT Model

With the use of video and recorded data from IMUs and LRF many aspects about assisted gait on slope have been observed. The main concept is that the human-robot interaction present with this kind of walkers on slope is very complex, because the user has to be free to move as he/she wishes and the walker has to achieve its goal, without limiting user intentions and never receiving direct inputs from him/her, such as the ones given through a joystick or a touchscreen. It is a matter of interpreting human movements and reacting consequently.

As explained in Chapter 4 the walker control strategy is based on two targets:

- Keep a constant distance between human and laser source mounted on the walker,
- Keep the parameter ϕ in 0, obtained from Equation.4.8.

The target of the controller have been modified for the presence of inclinations without introducing new parameters. This strategy resulted very flexible and rapid to implement in order to control the walker on slopes. The nature of the control still remained the same, for this reason the stability of the control is assured.

Human robot interaction on slope can be modeled as two bars, one representing the user and the other one the walker; the two bars are linked with a pivot fixed with the walker-bar at handlebar height. Moreover, the same model is taken into consideration to describe the user-walker system reaction to inclination in both pitch and roll angles.

In Figure. 5.1 and Figure. 5.2 two schemes of the human-robot interaction represented by the two axis and the pivot are presented, respectively in the pitch and roll inclination.

This model allows to analyze some very important features of human natural and controlled motion on slopes. Point P is the Pivot point, b and a are geometrical dimensions of the walker explained below. α is the pitch angle and γ is the roll angle of the walker.

First, it is intended that the user autonomously and rapidly compensates the presence of inclination bending its lower body, mostly with his ankle, in smaller part with knees and last with his back. In order to develop an easy-to-use model, we have approximated this attitude as if the compensation in presence of inclination was completely done by the ankle joint. This consideration let us assume that we can trace an always vertical line, representing the user's axis, that passes through point P at waist height on human body. The blue axis in Figure. 5.1 and 5.2 represents the always globally vertical axis of the user.

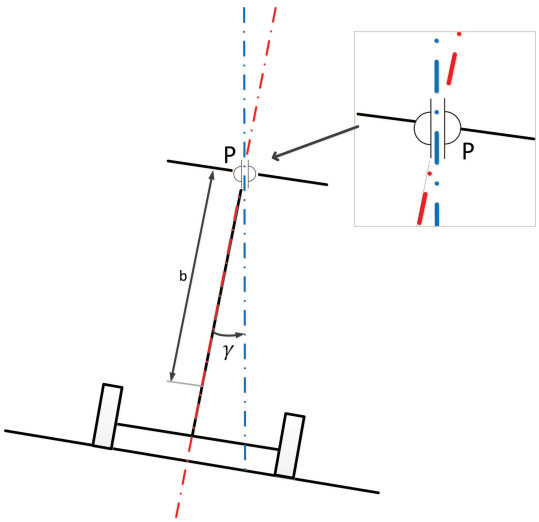

FIGURE 5.1: Scheme of the pivot model in the case of Roll inclination. In red the walker axis and in blue the User axis. With a close-up on the pivot.

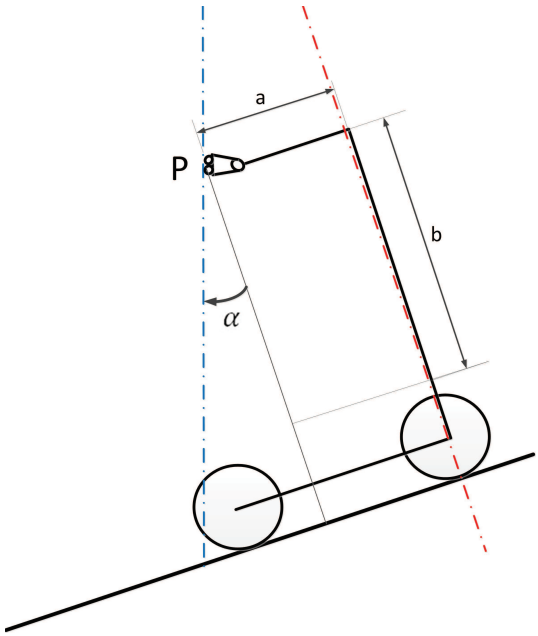

FIGURE 5.2: Scheme of the pivot model in the case of Pitch inclination. In red the walker axis and in blue the User axis.

Second, we simply assume that the walker always remains perpendicular to the soil, due to the good grip of the wheels and the limited velocity that doesn't permit any other orientation, consequent to phenomenon such as slipping For this reason we are able to draw a line, representing the walker's axis, always perpendicular to the soil, that passes through the handlebar and the on-board LRF, the red axis in Figure. 5.1 and 5.2.

In the next paragraph Figure. 5.1 and 5.2 will be deeply analyzed, referring to the indicated parameters.

The pivot is chosen to be the link between user and walker because it allows two desired movements:

- Rotation of the human axis, in order to remain always vertical, even if the walker rotates. This movement corresponds to the rotation done by the upper limbs, using a combination of muscles and joints.
- Shifting of the human axis in vertical direction, in order to have it's lower end always in contact with the soil. This corresponds to the fact that feet remain always on the floor. This compensation is also done by the upper limb.

Based on the video analysis resumed in Figure. 5.3, it appears a reasonable approximation to consider the waist height pivot point P as a point solidly fixed to the walker through the segment a for a kinematic analysis, even while on inclined planes. The length of the segment a, shown in Figure. 5.2 and 5.3 is supposed to be equal to the d_{cost} segment, set to $500mm$. The a_2 segment is the forearm support and is $330mm$ long; a_1 is considered to be equal to $170mm$ and it's the distance between the end of the forearm support and the pivot point P.

Data analysis done on one person $175cm$ tall are here presented to support the hypothesis done on forearm length a_1. The ratio $\frac{a_2}{a_1}$ in the 3 figures from left to right is: 1.9396 , 1.9677 , 1.9739. Obtaining an average of 1.9604. This value confirms the accurate estimated value of $a_1 = 170mm$ because from the two equations: $a_1 + a_2 = 500mm$ and $\frac{a_2}{a_1} = 1.9604mm$ it is obtained that $a_1 = 168.8961mm$.

From the orientation of the two axis, we determined the control parameters, that will be integrated with the ones obtained in the last version of the control strategy, which didn't take into consideration ground inclination: the method explained in Paragraph. 4.3.2. In the following two paragraphs the extraction of these parameters and their integration in the control is explained.

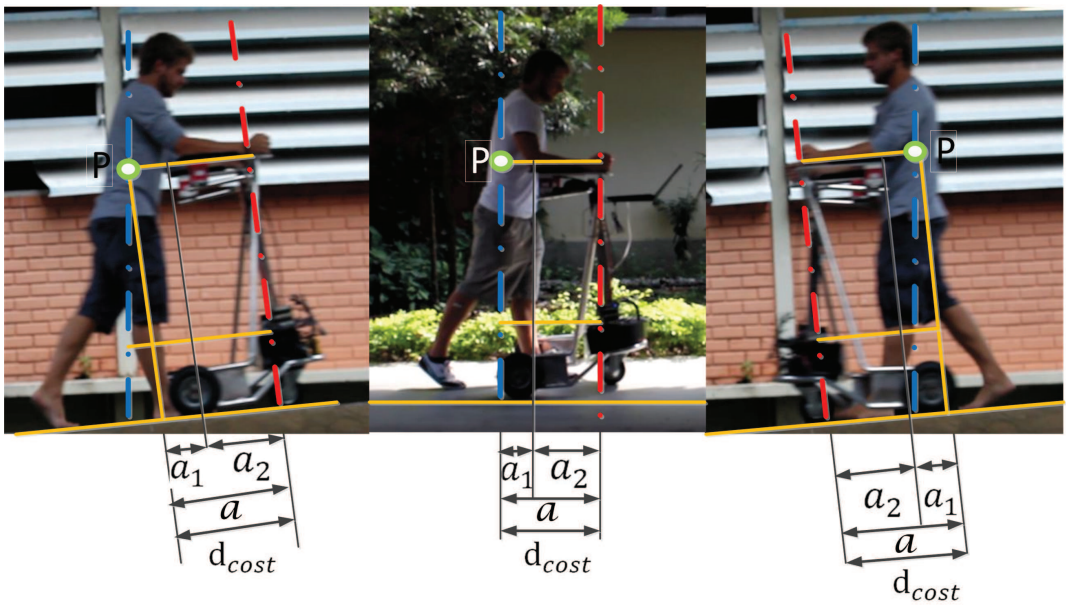

FIGURE 5.3: Pictures reporting human posture during assisted gait on slope. The red axis are representing the Walker axis, the blue ones the User, the green dot is the pivot point P and the yellow lines are construction lines. On the left the user is ascending the slope, on the center is walking on flat ground and on the right is descending the slope.

5.2 Pitch Model

In steady-state walker and user tend to have the same velocity, because the walker's speed depends on human's parameters which are constant when the user walks straight at a constant speed.

The described condition occurs when the user and the walker are on an horizontal ground or on the same inclined surface. Alternatively, when user and walker run on differently inclined planes the situation is more complicated. This happens when the walker encounters a variation in ground inclination, uphill or downhill and the user, which follows, is still on the previous condition, this results in an inevitable speed change of the walker.

Figure. 5.4 classifies the different sections of a ramp, differentiating the sections in which the walker and the user are not on the same plane. The complete ramp, that has a part going uphill and a part going downhill has been divided into 9 parts.

- A: user and walker on flat ground
- B: walker faces the uphill transition and user is still flat
- C: walker and user on the uphill slope

- D: walker returns on flat and user remains on slope
- E: walker and user on flat ground
- F: walker faces the downhill transition and user on flat
- G: walker and user on the downhill slope
- H: walker returns on flat and user remains on slope
- I: user and walker on flat ground

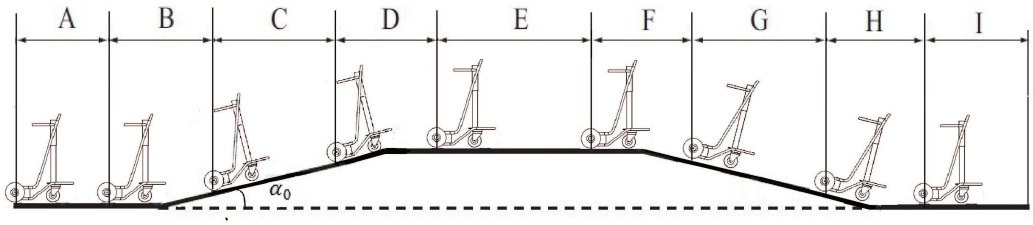

FIGURE 5.4: Different phases of the user-walker system in traveling throughout a slope.

On one hand, sections A, E and I correspond to the same condition of no slope, as well as phases C an G in which both the walker and the user are on the same slope.
On the other hand, sections B and H correspond to the same condition because the angle variation is positive in both cases, taken as a convention for α the counter clockwise direction, B going from 0 to a positive angle and H going from a negative angle back to 0. The same way sections D and F correspond to the same condition, a negative variation. Finally it's possible to define 3 possible conditions of the user-walker: on same slope, having a positive slope variation or having a negative slope variation.

The sections of ramp climbing in which the user and the walker are not on the same plane are now analyzed. Figure. 5.5 shows how the inclination of the walker changes when approaching a slope.

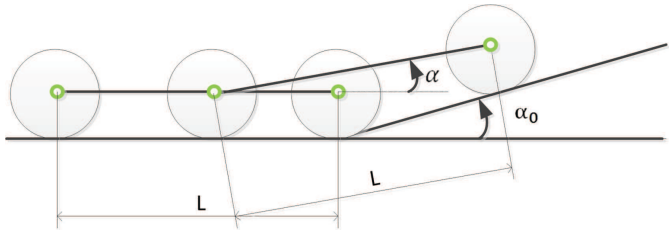

FIGURE 5.5: Scheme of the Walker approaching an inclined plane and while climbing the slope. α_0 is the slope angle and α is the pitch angle of the Walker

Few parameters are introduced: L is the length in between the front and rear wheel of the walker, α_0 is the slope of the ramp and α is the pitch angle read by the on-board IMU.

In Figure. 5.6 the angle α varies from null, when the walker is horizontal, up to the α_0 value when the walker is completely on slope. This variation, that happens both ascending and descending a slope, can be considered as a rotation of the walker. It is observable that the speed of the rear wheels v_r is still horizontal while the one of the front wheel v_f is inclined as the α_0 angle, from the intersection of the two lines perpendicular to the respective velocities, we encounter the instantaneous center of rotation O, around which the rotation happens.

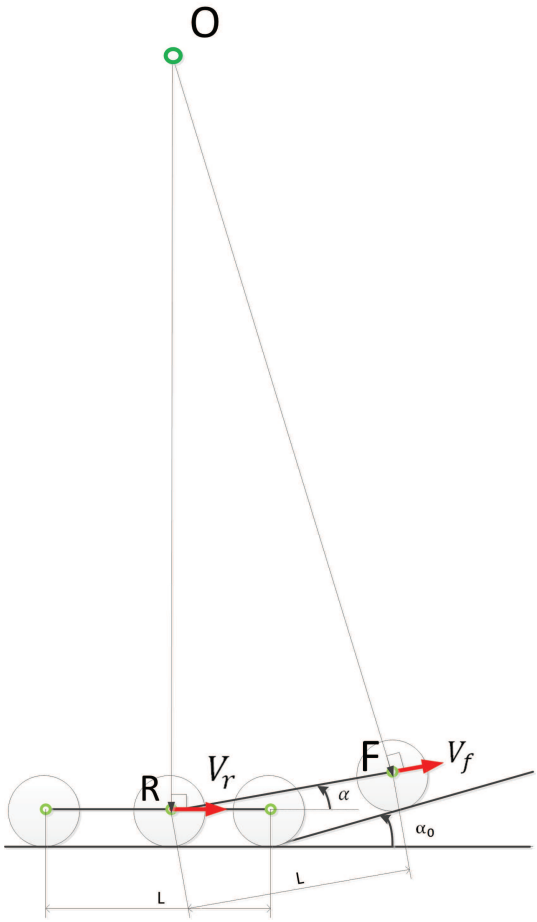

FIGURE 5.6: Scheme of the Walker approaching an inclined plane and while climbing the slope. In red are represented the speed of the rear (R) and front (F) wheels.

As shown in [47] the rotation, in a positive variation of inclination, results in a deceleration of the walker perceived by the user, because a component of the linear speed v_f is spent in the vertical direction. Practically, it results in an uncomfortable situation for the user because the handlebar gets closer to the waist and the user perceives the need

to push the walker harder, or lower it's speed. It is possible to conclude that, when in this condition, an increment in the traveling speed of the walker is desirable. The same reasoning can be applied to a negative variation of inclination: the handlebar gets far from the desired distance from the user and it results in the need of the user to pull the walker to reduce it's speed or the user has to walk faster. Therefore, it is desirable that the walker reduces its speed.

Generally, humans try to keep a constant speed while running on a slope [47]. To achieve this goal, not wanting to impose to the user any attitude and willing to develop a natural interface able to accompany the natural actions of the user, the control strategy modifies the walker's behavior when placed on a slope.

It is important now to define the concept of "load feeling" or "burden" meaning the perception of the user when using the walker, it can be defined as the amount of requested push to the user in order to keep it's desired speed. Commonly a good goal for slope compensation is to make the user feel as if he was on flat ground, meaning that even on slopes the burden perceived has to be constant [69].

It's a trend to use force sensors on smart walkers to have a control on the forces and torques exerted by the user and deal with the load feeling this way [70]. For example through an admittance model [71]. Unfortunately though the interpretation of the signal of the force sensors is not immediate. The force sensors can receive as input a certain signal that in different situations would have a different meaning, for example if the user would impart more strength in vertical direction it could mean that he needs more support, which makes the walker slow down, or that he is trying to acclerate the walker. These conditions would obviously generate different commands to the walker through a control strategy and can be easily confused.

In this case, a solution has been found in relation to the desired distance $\tilde{d}$. This signal is of much easier interpretation because the intention of the user or forward progression are expressed with an approximation to the walker and viceversa. The walker is programmed to keep a constant distance between the LRF and the middle point between user legs at LRF height. In order to assure a constant "load feeling" to the user, it's required that the distance between user and walker at the contact point in between them, the handlebar, remains constant. This means that the user tends, in all the conditions, to have the same amount of support from the walker and perceives the same need to push the walker. This results in a very dependable device that assures a constant support.

We have defined that the desired speed of the walker has to vary when it encounters a slope. When a positive variation of pitch angle occurs the speed required to the walker, in order to have a linear velocity at the handlebar equal to the one of the user, is higher

than the one it would usually have. For this reason the desired distance is raised during the evolution of the α angle, making the walker increment its speed to reach the desired distance. Symmetrically when a negative variation of pitch angle occurs the desired distance is reduced, making the walker decelerate.

In Figure. 5.7 the model is represented in the three conditions analyzed: when encounters a negative variation of pitch in Figure. 5.7(a), when encounters a positive variation of pitch in Figure. 5.7(b) and when remains on flat ground in Figure. 5.7(c). The hypothesis already introduced that distance a is constant and corresponds to the desired distance $d_{cost} = 500mm$, which is shown in Figure. 5.7(a), 5.7(b) and 5.7(c).

The effect of inclination visibly alters the user-walker distance in the proposed model, based on Figure. 5.7 the new desired distance is obtained as follows:

$$d_d = d_{cost} + d_p = 500 + b * \tan(\alpha) \tag{5.1}$$

b is the length between the handlebar and the laser source. d_{cost} is the constant value introduced in Chapter 4, usually set to $500mm$. d_p is the parameter that defines the component of the desired distance that depends on the pitch angle. d_d is the desired distance considered in the controller developed in this chapter.

The desired distance depends on the pitch angle, when the angle is null the desired distance d_d is equal to the constant value of $500mm$, as in the controller described in chapter 4, being the $tg(0) = 0$.

The modification introduced in the definition of the desired distance doesn't produce any major change in the program and doesn't interfere in the smoothness of the control law because it doesn't need switch to activate, but just the presence of a slope. In contrary, solutions as the one proposed in [47] multiply the velocity by a coefficient when in presence of slope. The coefficient is different accordingly to inclination's sign and absent when on flat ground, so the switch in between different conditions would produce irregularities in the control signal.

5.2.1 *CC*: Corrective Coefficient

In chapter 4 the corrective coefficient used to adapt the step amplitude to the real walked path was introduced. On slope, the behavior of this coefficient had to be studied. When the walker inclines, as shown in Figure. 5.3, the height at which the laser detects the legs shifts. Many tests with human linear speed set to 500 mm/sec have been analyzed and the maximum pitch angle rate usually found is approximate to $\dot{\alpha} = 3/sec$. Human

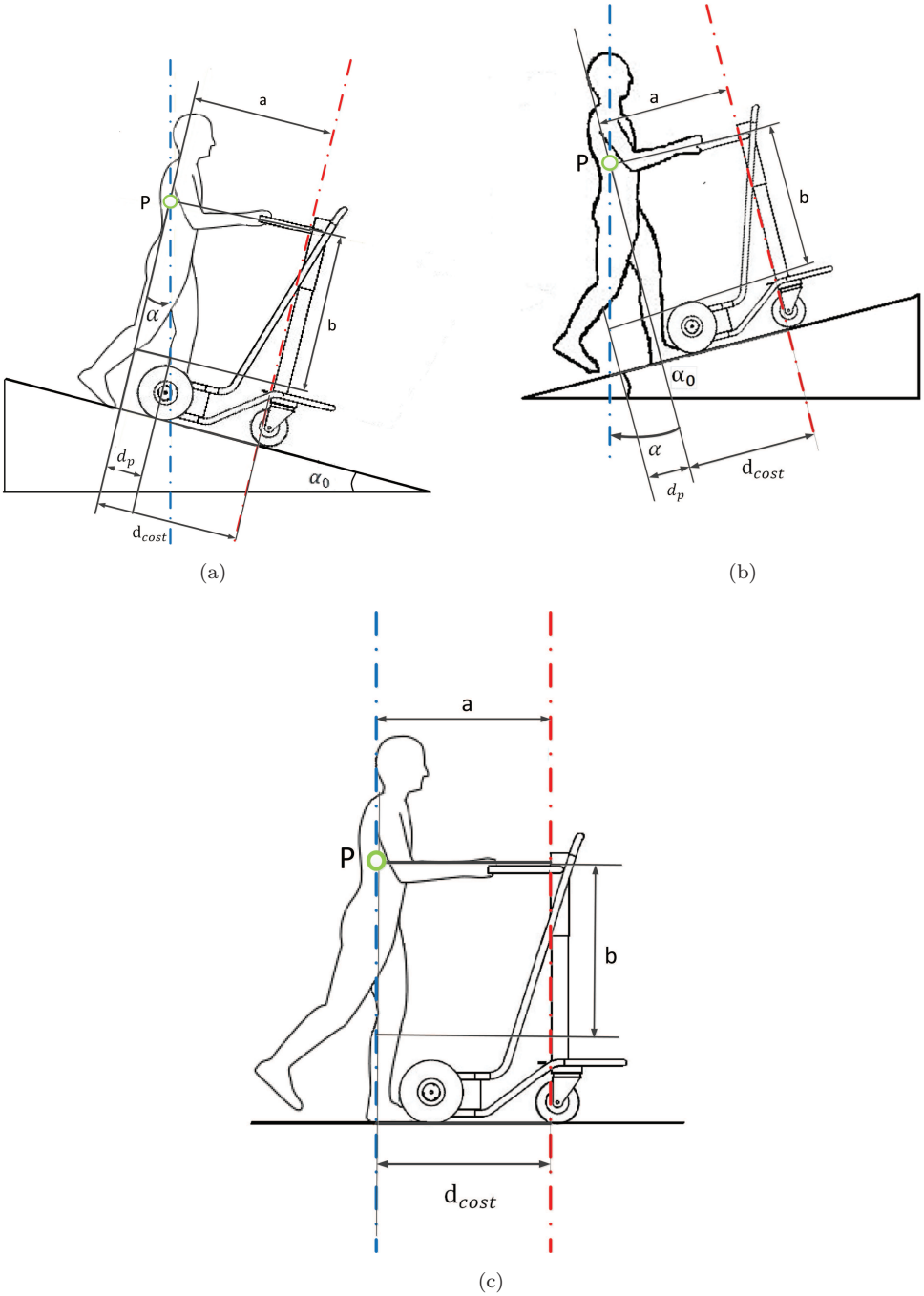

FIGURE 5.7: Human-Walker running downhill(a), uphill (b) and on flat ground (c). In red is represented the walker axis, in blue the human axis, the green circle is the fixed point P corresponding to the pivot.

linear velocity is set with the use of a metronome to pace each step and marks on the floor to determine step length, as done in the experiments of Paragraph. 4.3.3.2.

Table. 5.1 reports the data extracted from the video taken during tests and reveals the fact that the value 1.6 is a valid approximation for the CC also when the walker and the user are both on an inclined plane, in uphill and downhill condition.

In table. 5.2, there are reported some values taken from the analysis of images of user and walker while on differently inclined planes, specifically when the walker is completely on slope and the user is still on flat ground. In this condition, the influence of a modification to the CC is supposed to have a strong impact and effectively the data collected allows to define the maximum and minimum CC considered, $CC_{max} = 1.8$ and $CC_{min} = 1.4$. Values that differ from the usual 1.6.

Moreover, tests 2 and 4 estimate the CC from the image in which the walker is inclined and the user is on flat ground, but considering as if the walker was on flat ground. From the same picture is obtained the value of CC for the condition of walker and user both on flat ground and the condition of user and walker on differently inclined surfaces. In Figure. 5.8 test 1 and 2 are represented. Test 1 considers points: 1,2,3 and 4 while test 2 considers points 1,5,3 and 4. The obtained result is that when the two agents are both considered on flat ground the CC value is, as expected, 1.6.

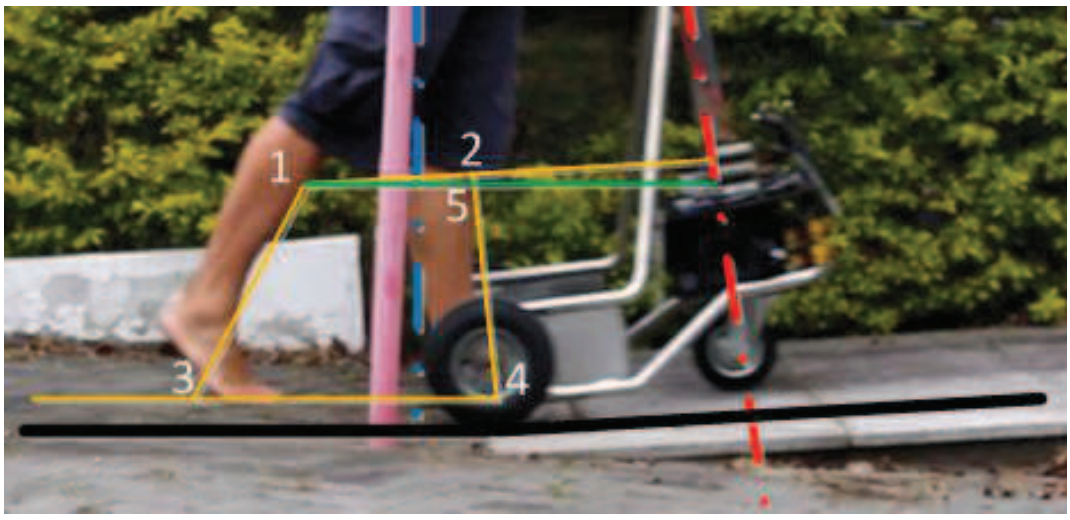

FIGURE 5.8: Image used to detect the CC in transitory conditions. Walker fully on uphill slope and User still on flat ground.

Equation. 5.2 has been defined empirically to determine the CC depending on the pitch angle, where the coefficient p needs to be estimated. This equation modifies the value of CC only when $\dot{\alpha}$ is different than 0; when pitch is constant, CC is still 1.6.

$$CC = 1.6 - p * \dot{\alpha} \tag{5.2}$$

Equation.5.2 is based on the idea that when the pitch variation is positive the coefficient CC is smaller, because the value read by the LRF is closer to the actual walked path at ground level and when the variation is negative the coefficient is higher. Replacing the maximum values defined for $\dot{\alpha}$ and CC_{max} it was found the value of $p = 0,067$, to check this value, the CC_{min} and p were substituted in the equation and the pitch angle variation was correct. Equation 5.2 has been implemented in the controller and online modifies the CC to better represent the real LRF readings.

5.3 Roll Model

Lateral inclination with respect to the heading direction in urban environment are very common, curbside is the setting in which it most occurs; this is because curbside lean street-side in order to let water drain. Moreover, the fact that a device is able to deal with lateral inclination come in support when a longitudinal ramp is climbed diagonally, requiring the use of a compensation both in the longitudinal and lateral directions.

Knowing the hypothesis made in this chapter regarding the imposed inclinations for user and walker axis on slope: walker always perpendicular to the soil and user always globally vertical and with the tentative to keep the pivot point P in the same location as in the Pitch Pivot model, the developed model for roll angle is now proposed.

Videos recorded during tests and data from the two IMUs were analyzed. It was observed that the user tends to compensate lateral inclinations mostly with his/her ankles, remaining in a vertical position with his/her trunk. In order to do so and to keep a comfortable position for arms and shoulders, the natural human reaction is to displace his/her feet laterally in direction of the lower side.

As shown in Figure. 5.9, the usual conventions are kept: in blue the user axis, in red the walker axis, length b is the distance between the handle-bar and the LRF, γ is the roll angle and f is the expected displacement of user's feet in the lower side direction, considered at LRF height.

The Pivot model is applied also in this situation considering point P as fixed to the walker centered at handle-bar height. The Pivot allows all the desired movements: relative rotation between user and walker axis and the shift of the user axis in order to remain always in contact with the ground.

Figure. 5.10 represents what has been discussed in this paragraph in a real test, it shows that the Pivot point P keeps an acceptably constant position between flat and inclined ground. Morevoer, user's feet are displaced in the expected direction.

TABLE 5.1: Values for *CC* extracted from picture analysis when Walker and User are both on slope.

Test		up left	up right	down left	down right	upper dist	lower dist	cc	Comment
1	x	120	216	82	240	96,62815	158,9119	1,644572	uphill, Walker and User fully on slope
	y	406	395	512	495				
2	x	150	250	115	280	100,4988	165,6804	1,648582	uphill, User and Walker fully on slope
	y	420	410	525	510				
3	x	180	275	155	310	95,52487	155,8236	1,631236	downhill, User and Walker fully on slope
	y	420	410	526	510				
4	x	215	304	200	350	89,14034	150,12	1,684086	downhill, User and Walker fully on slope
	y	400	395	506	500				

TABLE 5.2: Values for *CC* extracted from picture analysis when Walker and User are in transitory conditions: Walker on slope and User on flat ground.

Test		up left	up right	down left	down right	upper dist	lower dist	cc	Comment
1	x	105	195	70	198	90,55385	128,0039	1,413567	Walker uphill User flat
	y	310	300	405	406				
2	x	115	195	70	195	80	125,004	1,56255	Walker uphill (But considered flat) User flat
	y	300	300	405	406				
3	x	235	285	215	305	50,24938	90	1,791067	Walker downhill User flat
	y	265	270	365	365				
4	x	240	295	215	305	55	90	1,636364	Walker uphill (But considered flat) User flat
	y	275	275	365	365				

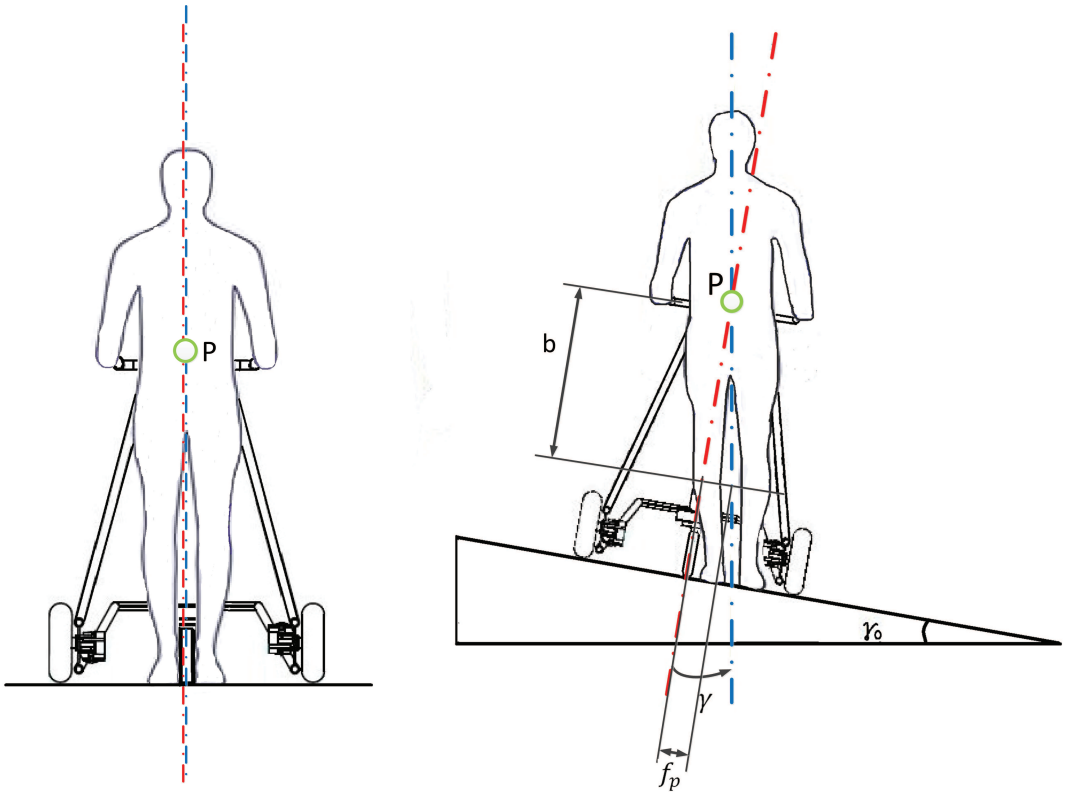

(a) (b)

FIGURE 5.9: Scheme of the pivot model in the case of Roll inclination. Human-Walker walking on flat ground(a) and on transversely inclined ground(b) In red the walker axis and in blue the user axis.

From kinematics extracted from Figure. 5.9, the f distance, based on the roll angle γ, is obtained and shown in Equation. 5.3.

$$f_p = b * \tan(\gamma) \tag{5.3}$$

The extracted value f_p is the desired value of lateral displacement when in presence of a γ roll inclination angle. In the case of no lateral inclination the parameter f_p is null, because $\tan(0) = 0$.

From another perspective the displacement described is extracted with other parameters, Figure.5.11 shows an upper view over user and walker. The position of the middle point between user's legs H with respect to the walker W is described by two parameters: distance d and angle θ both read by the LRF placed on-board.

It is necessary to elucidate the meaning of the parameters shown in Figure.5.11.

- v_w and ψ_w, in red, are respectively the walker's linear velocity and its orientation;

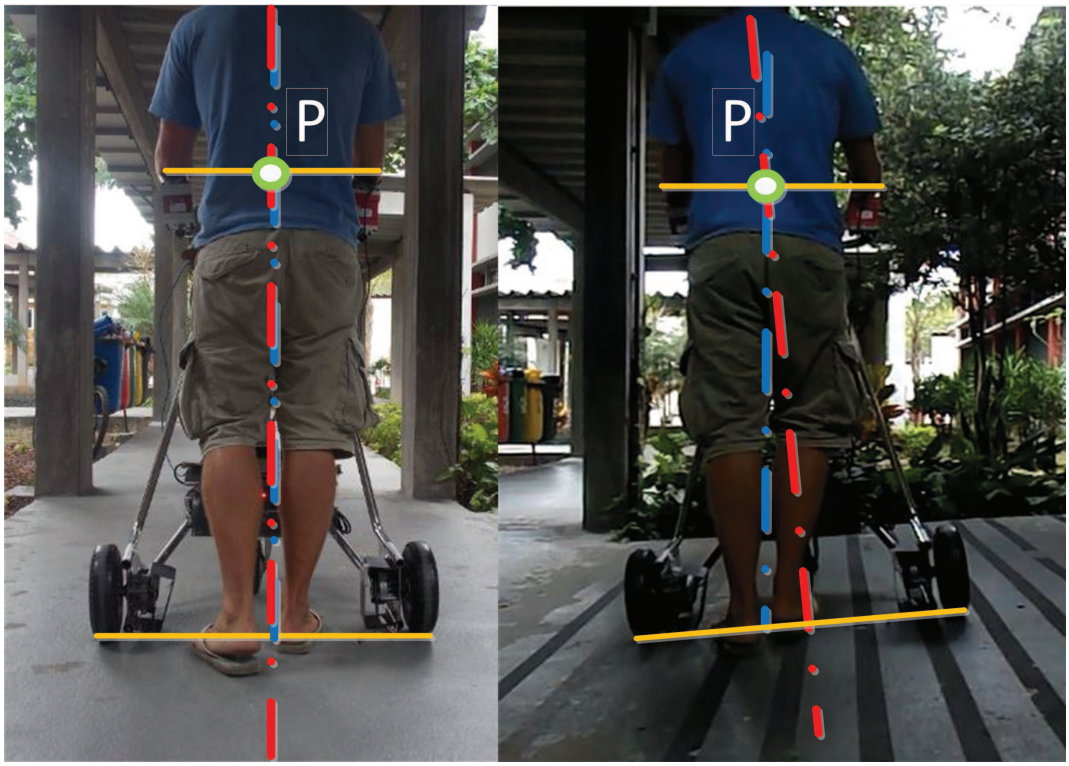

FIGURE 5.10: Pictures of the pivot model in the case of Roll inclination. In red the walker axis and in blue the user axis. On the left on flat ground and on the right on inclined ground.

- v_h and ψ_h,in blue, are respectively the user's linear velocity and its orientation;
- d is the distance between point W and H;
- θ is the angle between the walker velocity vector v_w and the segment connecting points H and W. This parameter is the orientation of point H, the middle point between human's legs, seen from point W, which corresponds to the LRF on-board;
- the angle φ is the angle used in the control defined in Equation. 4.8 and reported here in Equation.5.4;

$$\varphi = \theta - \psi_w + \psi_h \tag{5.4}$$

- f is the lateral displacement of the middle point between user's legs, in direction perpendicular to walker's axis and is extracted with Equation. 5.5, which is obtained from Figure. 5.11;

$$f = d * \sin(\theta) \tag{5.5}$$

- f_p is the parameter extracted in Equation. 5.3 and is the desired value of lateral displacement. This parameter can be expressed also with Equation. 5.6, function of θ_p;

$$f_p = d * \sin(\theta_p) \tag{5.6}$$

- θ_p is the angle that produces a lateral displacement equal to the desired value f_p. When no lateral inclination is present this angle is null because the f_p is null, due to γ being null;

  Inserting Equation. 5.3 into 5.6 Equation. 5.7 is obtained, this equation is used to extract the desired θ_p.

$$\theta_p = \arcsin(\frac{b}{d} * \tan(\gamma)) \tag{5.7}$$

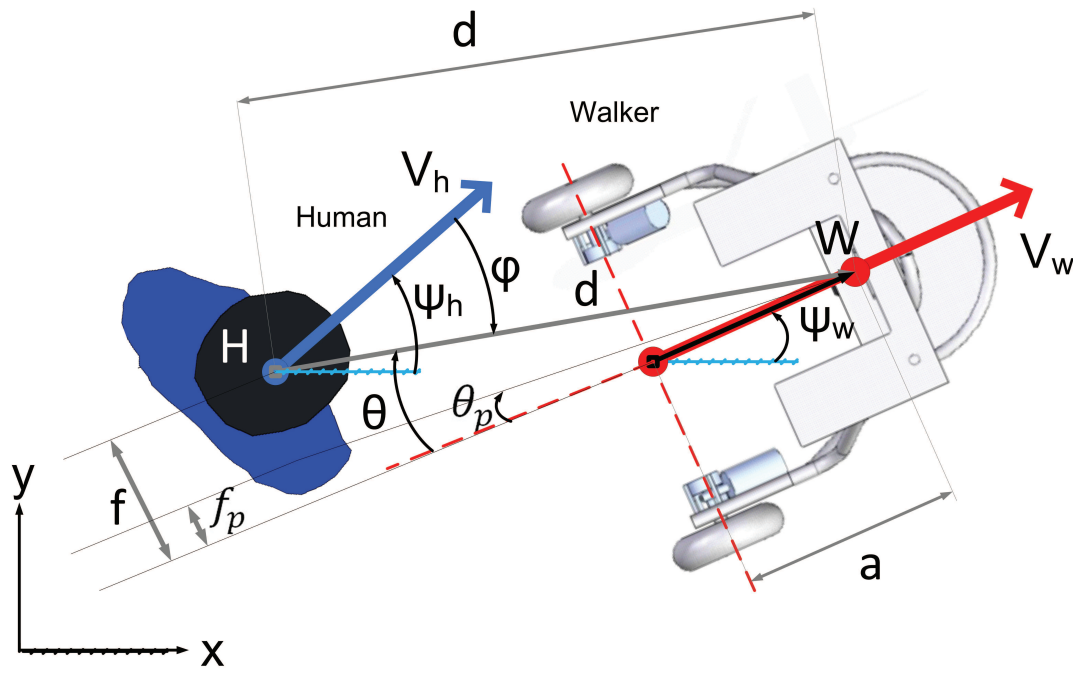

FIGURE 5.11: Upper view in the x-y plane of the user walker model in the case of roll inclination. In red the walker's linear velocity and in blue the user's one.

When on lateral slope, the displacement f_p of the middle point between user's feet in the lower side of the slope is a natural reaction, confirmed by picture analysis. Natural reactions of the user to a certain situation are considered conditions to be achieved in the controlled motion. For this reason the controlled motion on laterally inclined ground modifies the target of the control strategy. From this analysis, it was obtained that in order to keep the walker in a comfortable condition for the user the target for the control parameter φ had to be changed from 0 to θ_p.

Recalling that the domain of Arcsin is $[-1;1]$ and that its range is $[-90;90]$. On one hand, the range is satisfactory because the desired θ_p is surely included in it. On the other hand, the domain had to be studied. The argument of the Arcsin has to respect the domain limitation, $-1 < \frac{b}{d} * \tan(\gamma) < 1$. Considering a minimum accepted distance of $200mm$ and the constant value of b the disequation simplifies in $-14.57 < \gamma < 14.57$. This means that in order to have the control working correctly the roll angle γ is limited and the distance d has to be greater than $200mm$. Both of the condition don't interfere with the normal functioning of the walker.

In the case shown in Figure.5.12 the two orientation ψ_r and ψ_h subtracted one to the other result in 0, considering the two velocities v_h and v_r parallel. So, in this condition, Equation.5.4 reduces into $\varphi = \theta$. In this condition is easier to picture the fact that the control has to achieve the condition of $\varphi = \theta_p$ as target.

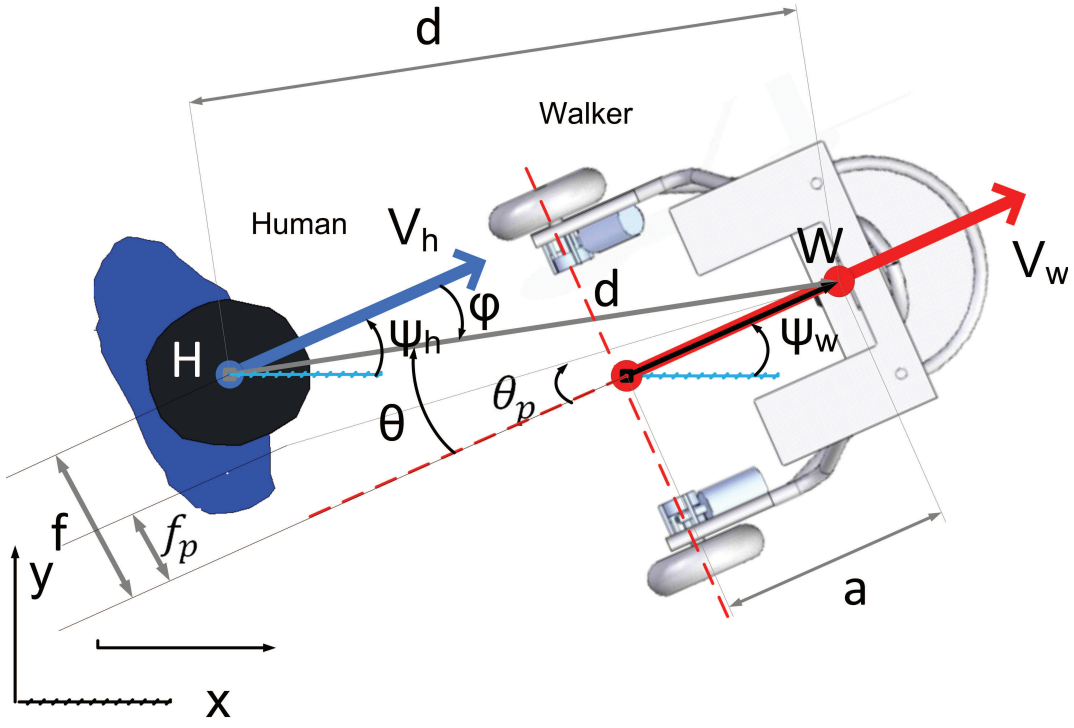

FIGURE 5.12: Upper view in the x-y plane of the user walker model in the case of roll inclination. In red the walker's linear velocity and in blue the user's one.

The variation in the corrective coefficient CC is not taken into account when treating roll inclinations because of it's very limited variation.

5.4 Supervisor Block: the Pivot model

The kinematic analysis developed in sections Pitch Model 5.2 and Roll Model 5.3 was integrated in the closed control loop, as shown in Figure. 5.13.

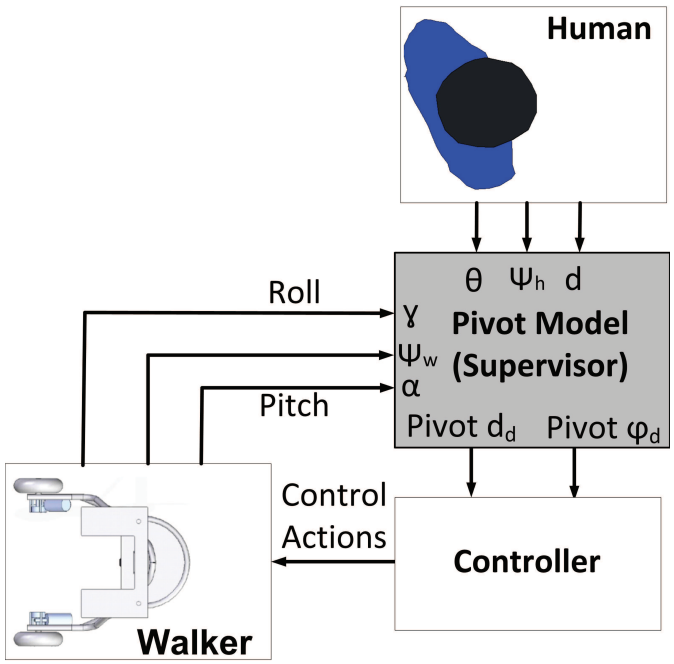

FIGURE 5.13: Block diagram of the Pivot model, the supervisor block.

The input defined in this model come from human localization (θ,ψ_h and d) and from walker orientation (ψ_w, Roll- γ and Pitch- α). The outputs are the Pivot d_d and the Pivot φ_d that represent the adjusted set points entering the controller in order to close the control loop. Finally the control actions are fed to the walker.

5.5 Conclusions

The Pivot model successfully uses the pitch and roll angles, detected by the IMU on-board, to adapt the control strategy to an environment with inclinations: longitudinal and lateral.

Video analysis shows a similarity between the real position of segments of human body and the proposed model. Moreover, in accordance with the hypothesis done in the model the walker remains always perpendicular to the ground.

The walker roll and pitch are signals with a principal component due to the orientation of the walker, a component due to human cadence and a noise component due to the

oscillation of the mechanical structure for soil irregularities and imperfections in the wheels. For these reasons the Roll and the Pitch signals have been filtered with a digital low-pass filter, implemented in MATLAB through the *FilterDesignandAnalysisTool*.

The scheme proposed in Figure. 5.14 is the complete logical scheme that introduces the walker's pitch and roll angles into the control strategy; it is a complete version of Figure. 4.3.4 deeply commented in paragraph 4.3.4.

A remarkable aspect of the developed control strategy is that when running downhill the user is not required to worry about pulling the walker in order to keep it from rolling away. Furthermore, he doesn't have to push it, as it's required when approaching the inclination problem with an admittance model, as found in [47].

Finally, no need of training is required to use the UFES smart walker with the proposed controller, because the input required by the controller corresponds to the natural attitude that a person has on slope.

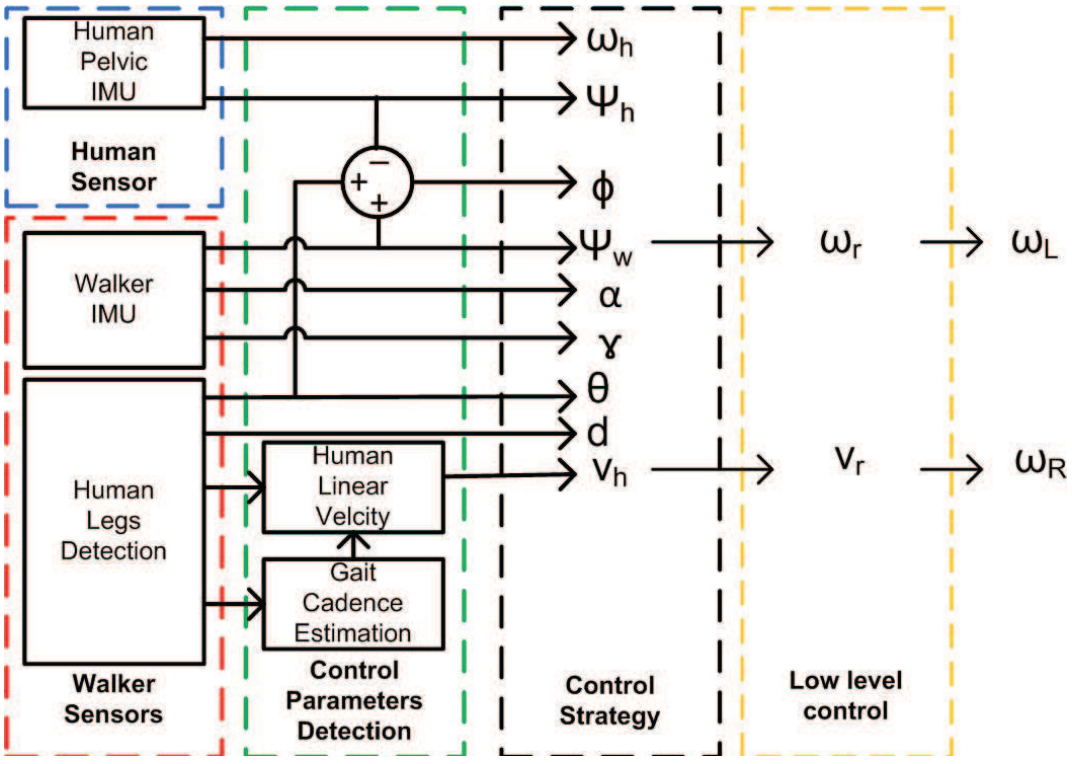

FIGURE 5.14: Scheme of the multimodal fusion of sensors: the IMU on human and the IMU and the LFR on the Walker. With the introduction of Pitch and Roll angles. From sensors to actuators

Chapter 6

Experimental validation

In order to validate the Pivot Model proposed in chapter 5 a set of experiments has been developed. A healthy subject without any locomotion-related problems of height 175 cm volunteered to perform the experiments.

Due to technical problems at the moment of experimentation the IMU positioned on the user was not used. Due to this limitation the Yaw angle of the user was not available. For this reason the control strategy was modified not to depend on this parameter. Equation. 4.8 can be simplified not considering the human yaw ψ_h and walker yaw ψ_w, reducing from $\varphi = \theta + \psi_h - \psi_w$ to $\varphi = \theta$. All the experiments presented in this chapter use as control parameter θ and not φ.

Tests have been done without control, which means that the motors were disconnected from the axis of traction during the experiment. The purpose of these experiments was understanding the natural interaction between human and walker on slope. Without a controlled motion of the walker the user just receives a passive support and autonomously positions him/herself in a comfortable position. The need to push and secure the walker, which is free to move, requires an effort to the user in order to maintain the desired motion. Offline a confrontation between the natural user-walker interaction and the target values of the control strategies has been done. The control strategy presented in chapter 4, which will be called Normal strategy, and the Pivot model control strategy presented in chapter 5, which will be called Pivot strategy, have been compared in relation to the natural interaction. In this set of experiments have been used the linear path and the U-shaped path, shown respectively in red and black dashed lines in Figure. 6.1. The tests are explained in Paragraph.6.3 and 6.4.

FIGURE 6.1: Representation of the paths used in the experiments. In red dashed line the Linear path and in black dashed line the U-shaped path.

6.1 Experimental setup 1: Linear path

Figure. 6.2 shows the different sections of the linear path on slope, which in this case is climbed uphill. The path begins with a horizontal section of 2 meters, followed by a +4° longitudinally inclined section of 9 meters and ended by another horizontal section of 4 meters. The candidate was asked to perform the linear path uphill while guiding the walker.

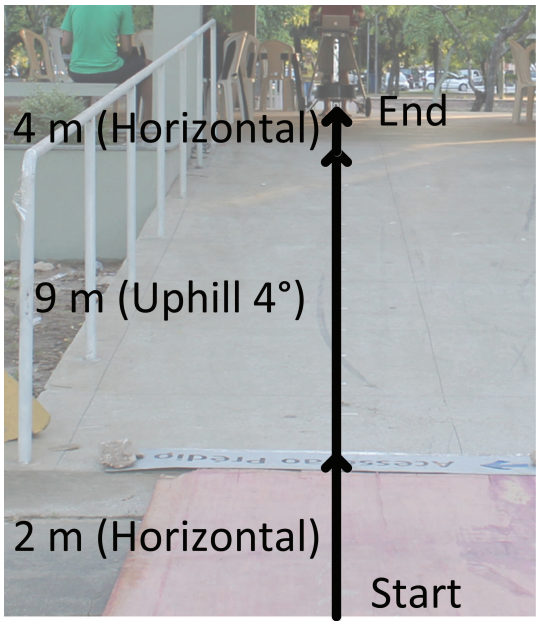

FIGURE 6.2: Linear path on longitudinal slope.

6.2 Experimental setup 2: U-shaped path

Figure. 6.3 shows the different sections of the U-turn path on slope. The path begins with a horizontal section of 2 meters (first black solid line in Figure. 6.3), followed by a $-4°$ longitudinally inclined section of 2 meters (first grey solid line in Figure. 6.3), then comes a U-turn (black dashed line in Figure. 6.3), composed by two left turns and a short, 1 meter long, section of laterally inclined path, a $+4°$ longitudinally inclined section of 2 meters (second grey solid line in Figure. 6.3), and a horizontal final section of 2 meters (second black solid line in Figure. 6.3). The candidate was asked to perform the U-turn path while guiding the walker.

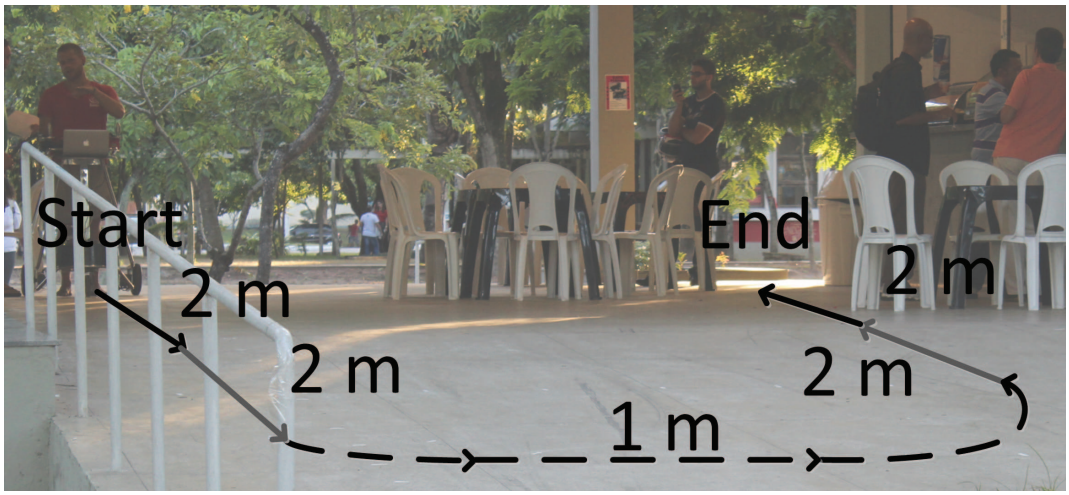

FIGURE 6.3: U-turn path on longitudinal and lateral slope..

6.3 Results of experiment 1: Linear path

Figure. 6.4 reports few important parameters of this experiment, which has been done with a pace of $1 step/second$ regulated with a metronome and with step length of $500mm$ marked on the floor with tape. Figure. 6.4e shows the estimation of the linear velocity obtained with the technique explained in chapter 4, resulting almost $0.5m/s$.

In Figure. 6.5a are shown the values of distance read by the LRF for right and left leg respectively in black and grey and their average value in red. In Figure. 6.5b it is possible to appreciate the variation of the walker pitch signal, confirming that the path was crossed uphill, showing a positive variation up to $+4°$, a constant section in which the walker is on slope, a negative variation which brings the pitch back to almost $0°$ and a last section on horizontal ground. Moreover,in Figure. 6.5c are represented 3 signals of distance between the center point of user feet and the LRF: the actual human distance

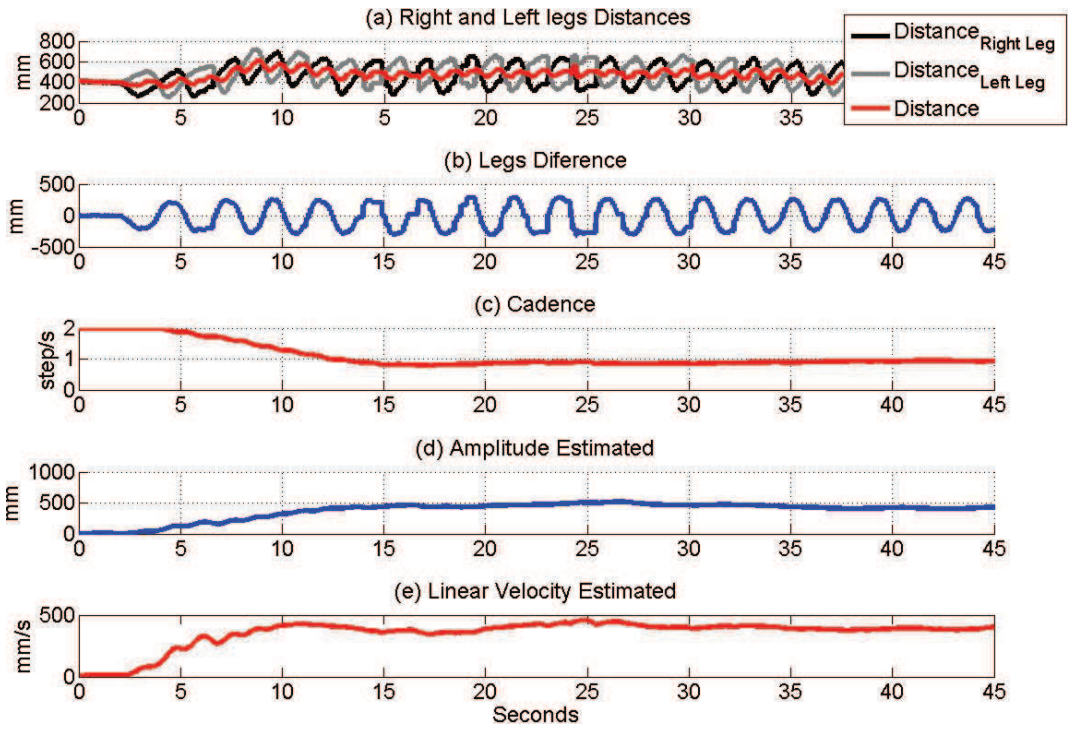

FIGURE 6.4: Parameters of the march. (a) Right and left legs distances in red and green respectively, with their average in black. (b) The difference of the two legs distances. (c) The estimated step cadence. (d) The estimated step amplitude. (e) The estimated linear velocity.

d in red, the desired distance obtained with the Normal controller, Normal d_d, in blue, and the desired distance obtained with the Pivot model, Pivot d_d, in black.

In Figure. 6.5c the real distance d and the Pivot d_d have a similar trend in their evolution, different from the Normal d_d, which is constant. In this work the author assumes that if, in an experiment performed with no controlled motion, the value to be controlled and the control set point present a similar trend, the system, once controlled with this setpoints, would present a natural behavior, as explained in chapter 5.

Furthermore, the actual distance d results smaller than the Pivot model desired distance, Pivot d_d. This phenomenon is mostly due to the fact that the Pivot model desired distance is just an estimation of the natural distance that the user would keep from the walker on slopes. Partly though because in uphill situations and without control the user finds him/herself closer to the walker than what would be the most comfortable position, since in need to push it.

At the beginning of the slope, the real distance shows an unexpected behavior: increasing up to $600mm$ to rapidly decrease to $500mm$, which is the distance at which the user runs when on this slope. This phenomenon is due to the position that the user has when

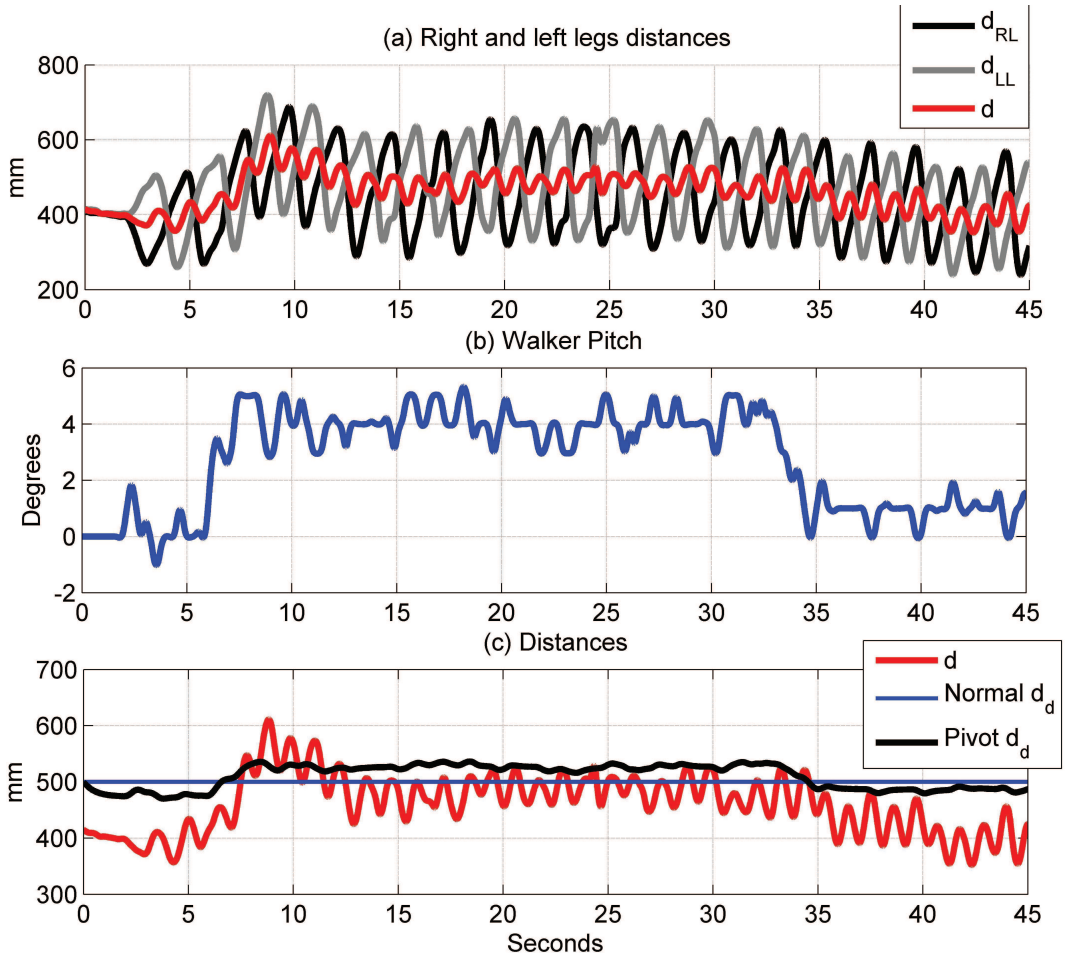

FIGURE 6.5: (a) walker pitch signal. (b) Legs distance in red, desired distance of Normal method in blue and desired distance of Pivot method in black.

begins to push the walker uphill. In order to generate the necessary pushing force, the user inclines his body and brings his feet farther from the walker.

Figure. 6.6a and b represent respectively the parameter $\tilde{d}$ found with the use of the Pivot method and with the Normal method and the walker pitch signal is represented in Figure. 6.6c.

It's useful to recall that $\tilde{d} = d - d_d$. $\tilde{d}$ is the difference between the real distance and the desired distance, this parameter is an input to the control block. On one hand, in Figure. 6.6(a) the $\tilde{d}$ oscillates around a stable negative value, even when the walker runs on slope. If fed to the control, this signal would produce a limited effort of the controller, by the fact that the error doesn't have strong variations. Merely in the section of approaching the slope the error grows, but as previously explained this is due to the lack of control.

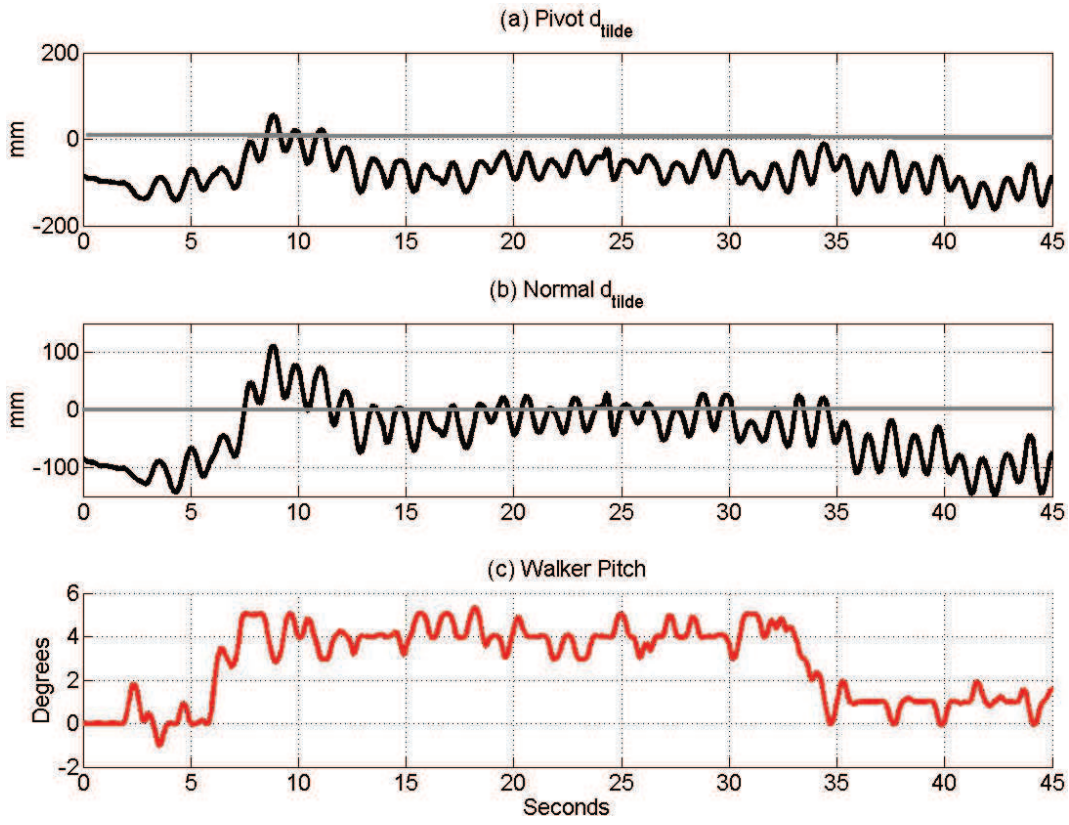

FIGURE 6.6: Analysis of the $\tilde{d}$ parameter variation with the Pivot model. (a) $\tilde{d}$ obtained with the Normal model. (b)$\tilde{d}$ obtained with the Pivot model. (c) Walker pitch signal.

On the other hand, in Figure. 6.6(b) the $\tilde{d}$ has a trend that depends on the inclination, it does not oscillates around a value. If fed to the control, this $\tilde{d}$ would try to compensate the distance variation that naturally happens when running on slope, producing a less natural control strategy.

6.3.1 Corrective Coefficient

The proposed experiment has been used to validate the model developed for the Corrective Coefficient (CC) variation on slope of Equation. 5.2 introduced in chapter 5. Figure. 6.7a represents the walker pitch angle. Figure. 6.7b shows, in red, the CC obtained with the Pivot model CC correction and, in blue, the CC used in the Normal model, constant at value 1.6. The CC from the Pivot model has two significant variations. The first corresponds to the beginning of the uphill motion of the walker, a positive variation of the pitch angle, resulting in a reduction of the CC. The second one corresponds to a decrease in the pith angle, being the section at which the slope ends resulting in an increase of the CC.

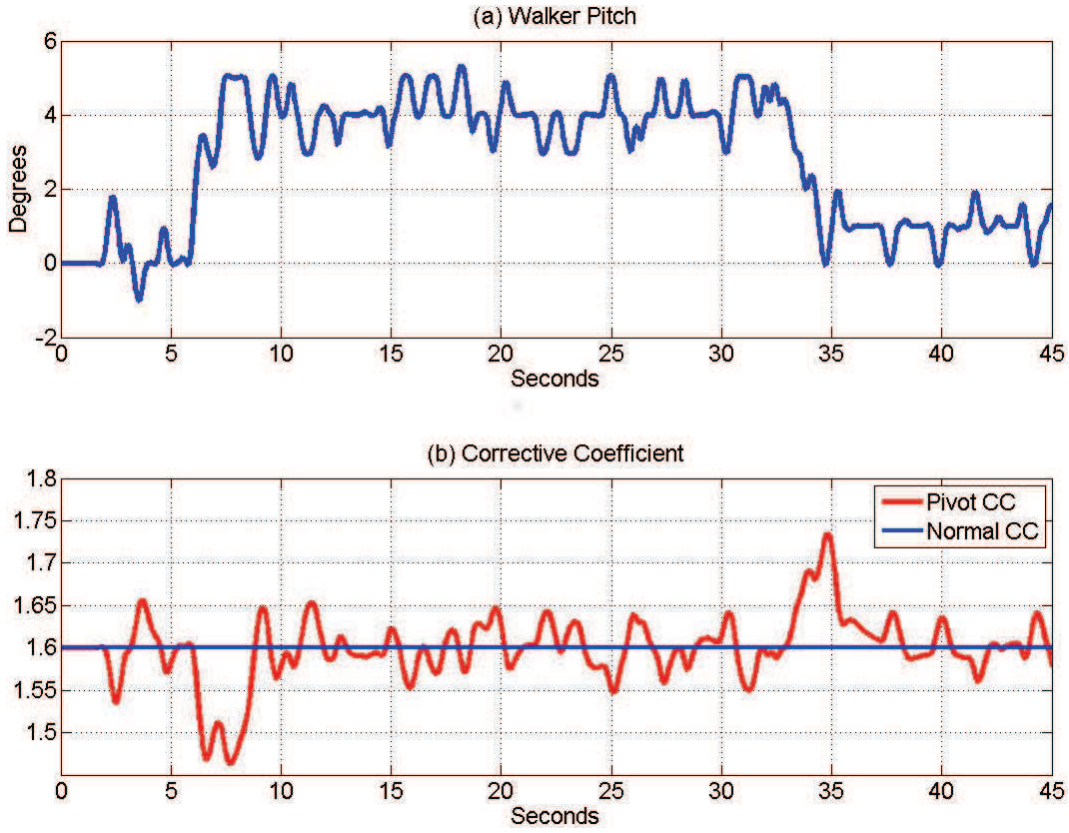

FIGURE 6.7: Analysis of the CC parameter variation with the Pivot model. (a) Walker pitch signal. (b) *CC* obtained with the Normal model in blue and with the Pivot model in red.

The experimental result are in line with the theoretical model developed for the CC variation on slope. The analyzed coefficient compensates the error of height at which the LRF reads legs parameters. In this experiment it is not possible to appreciate a significant improvement in the estimation of the amplitude, with the modification of the CC.

6.4 Results of experiment 2: U-shaped path

As explained in the previous paragraph, also this experiment has been done without control and has the goal to prove a similarity in between the natural behavior of the user and the estimated control target calculated through the Pivot Model.

The experiment has been done with the same step amplitude used for the experiment set 1, fixed to $500mm$, described in paragraph 6.3, and a cadence of $2step/second$. Because a too low speed would make a harder task to perform curves on inclinations without the assistance of the motors.

In Figure. 6.8 it's possible to define 5 different phases in the evolution of the trial. Approximately every two seconds of the test it is defined a new phase. Phase I is between seconds 0 and 2 and corresponds to the first black solid line in Figure. 6.3. Phase II is between seconds 2 and 4 and corresponds to the first grey solid line in Figure. 6.3. Phase III is between seconds 4 and 6 and corresponds to the black dashed line in Figure. 6.3. Phase IV is between seconds 6 and 8 and corresponds to the second grey solid line in Figure. 6.3. Finally, phase V is between seconds 8 and 10 and corresponds to the second black solid line in Figure. 6.3.

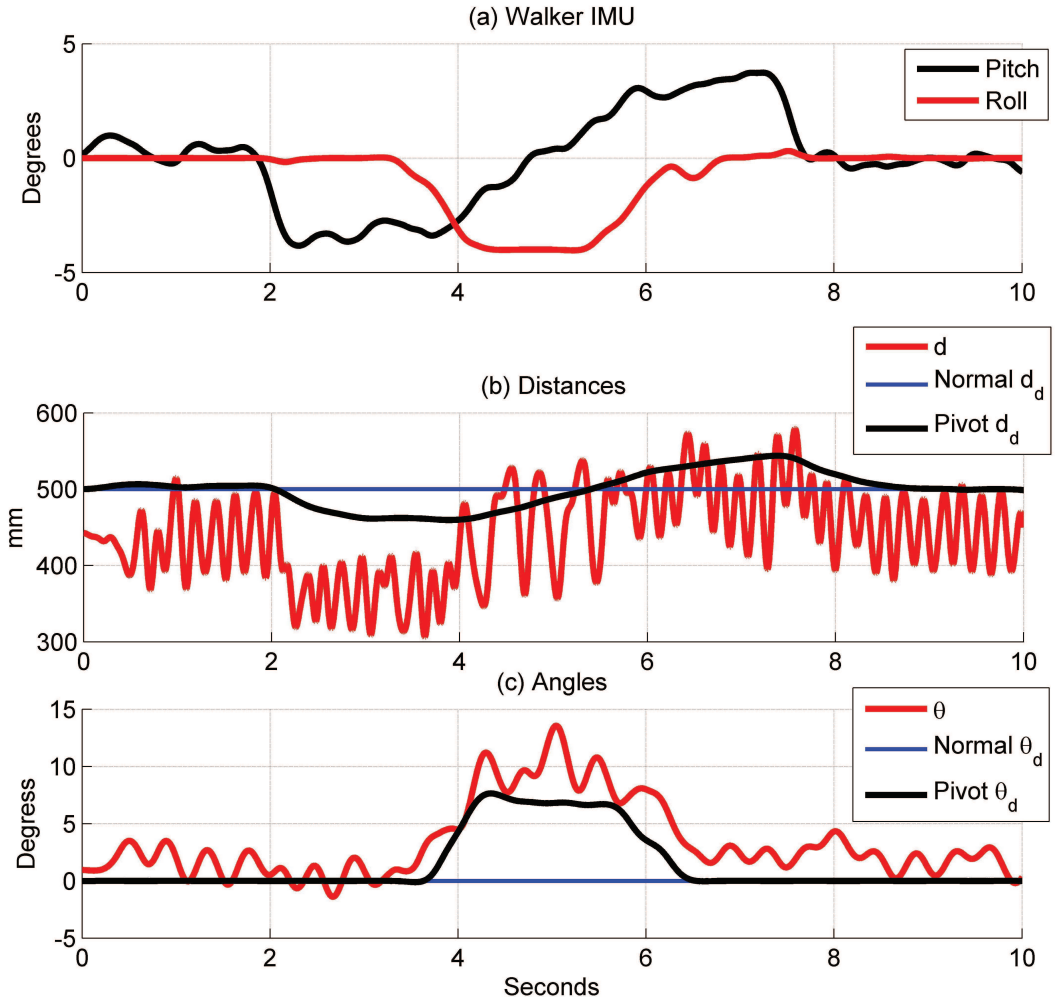

FIGURE 6.8: (a) Walker pitch and walker roll signals. (b) Legs distance in red, desired distance of Normal method in blue and desired distance of Pivot method in black. (c) Theta in red, desired theta of Normal method in blue and desired theta of Pivot method in black.

Phase I is on horizontal flat ground. This phase is characterized by a null pitch and roll angles, an almost constant distance d around value 450 mm, Normal d_d and Pivot d_d at value $500mm$ and almost null angles θ, Normal θ_d and Pivot θ_d.

Phase II is on the downhill slope. The pitch angle drops to $-4°$, and the roll angle keeps being null. The θ, the Normal θ_d and the Pivot θ_d remain in almost $0°$. d decreases of approximately 100 mm and keeps a constant value for the rest of the phase. The Pivot d_d also decreases of around 50 mm with the same trend as d, while the Normal d_d keeps its constant value of 500 mm.

Phase III is the phase in which the pitch angle returns to being null while performing the first part of the U-turn, remains in $0°$ during the laterally inclined section and increases up to $+4°$ completing the second turn of the U-turn. The distance d and the Pivot d_d evolve similarly incrementing respectively by 200 mm and 100 mm. The roll angle decreases up to $-4°$ during the first turn, maintains this value for the laterally inclined path and goes back to value $0°$ after the second turn. The θ and Pivot θ_d both increment with a similar trend, respectively up to almost $10°$ and $7°$, with the first turn, keep this value on the laterally inclined path and go back to $0°$ with the second turn.

Phase IV is on the uphill slope. The pitch angle increases to $+4°$, and the roll angle keeps being null. The θ, the Normal θ_d and the Pivot θ_d remain in almost $0°$. d oscillates but keeps an average value of approximately 550 mm for the rest of the phase. The Pivot d_d keeps its value of 550 mm with the same trend as d, while the Normal d_d keeps its constant value of 500 mm.

Phase V, as phase I, is on horizontal flat ground. This phase is characterized by a null pitch and roll angles, an almost constant distance d around value 450 mm, Normal d_d and Pivot d_d at value 500 mm and an almost null angle θ, Normal θ_d and Pivot θ_d.

In the different phases the parameters d and Pivot d_d evolve with a similar trend. In the same way, parameters θ and Pivot θ_d evolve with a similar trend. This behavior and the one observed in the first experiment, explained in paragraph 6.4, show the effectiveness of the Pivot model in defining the parameters Pivot d_d and Pivot θ_d, which can be used as set points for a control scheme in order to develop a natural and safe control strategy, as shown in Figure. 5.13.

Chapter 7

Conclusions, contributions and future directions

7.1 Conclusions

The presented thesis has the objective of developing a control strategy specifically thought for when the *UFES smart walker* runs on slopes: ramps and curbsides. The need of this research has appeared because smart walkers should be able to safely deal with inclinations in order to become a device effectively useful in the daily life of the elderly population or of anybody that suffer of limited mobility. In urban environments smart walkers very commonly have to deal with ramps and curbsides and the UFES smart walker was not prepared to safely face them.

This thesis presents the conception, development and validation, with a sane subject, of a novel model of human-walker interaction on slopes. This model is called "Pivot Model" and is based on the kinematic analysis of human posture during walker assisted-gait on slopes.

The developed model was integrated, as a supervisor block, into the conventional closed control loop implemented in the smart walker embedded hardware. This block modifies, depending on inclinations, the control set points to provide an adaptable human-walker desired position in order to improve comfort and safety and enhance user's confidence in the walker. The parameters used in the model are the legs position and the 3D orientation of the walker.

The experimental validation of the Pivot Model showed that the parameters extracted from the natural behavior of the user and the estimated set points determined with the Pivot Model are highly correlated presenting a similar trend in their evolution in time.

This behavior shows the effectiveness of the model in defining the control parameters, which can be used as set points for a control scheme in order to develop a natural and safe control strategy.

One of the advantages of the proposed method is the high computational efficiency, due to the light weight of the introduced algorithm. The estimated parameters don't present a considerable increase in the execution time and for this reason the Pivot Model is suitable for real time applications.

In literature no work has been identified in which the kinematic modeling of the human natural attitude on slope was considered in the definition of the control strategy. For this reason the proposed method is considered an innovation.

Moreover, the sensors taken into account in this configuration of the system are easily interpreted. The LRF data shows the actual distance and orientation of the lower limbs and the IMUs data show the orientation of the human pelvis and of the walker. This fact is noteworthy because other sensors are of more difficult interpretation, such as force sensors to measure upper limbs. The force sensors can receive as input a certain signal that in different situations would have a different meaning, for example if the user would impart more strength in vertical direction could mean that he needs more support, which means slow down the walker or that he is trying to accelerate the walker. These conditions would obviously generate different commands to the walker through a control strategy and can be easily confused. In the configuration used in this thesis this problem is not relevant.

For reasons of comfort and safety it has been defined a walkable space inside of which the user has to be encountered in order keep the motors turned on. This square space is limited by the mechanical structure in three sides and on the open side it is fixed at $1m$ the maximum distance that the LRF can detect.

Due to the clear interpretation of the sensor's signals, the limitations used in defining the walkable space and the self-blocking gear of the motors that block in emergency situations the control strategy is considered safe.

Finally, a great quality of the proposed control is the fact that no training is required in order to use the UFES smart walker. The input required by the controller are extracted from the natural attitude that a person has on slope.

7.2 Author contributions

As a master thesis a series of scientific contributions have been produced in the topic of walker-assisted gait. These contributions are listed as follows:

- Participation in the development of the final state of the *UFES Smart Walker*, a prototype and for this reason often in need of reparations and improvements.
- Participation in the definition and validation of the estimation strategy for the linear velocity of the user, fully explained in chapter 4.
- The study and critical review of the state of the art about mobility assistive devices on slopes, especially focusing on the theme of smart walkers.
- The conception, implementation and validation of the Pivot Model, in its subsections Roll and Pitch Models, fully explained in chapter 5 and 6.

7.3 Publications

RODRIGUEZ, C. A. ; CIFUENTES, C. ; **TAUSEL, L.** ; FRIZERA, A ; BASTOS, TEODIANO FREIRE. Estimação de Velocidade Linear em Marcha Assistida por Andador Utilizando Varredura Laser. In: VII Congreso Iberoamericano de Tecnologías de Apoyo a la Discapacidad - IBERDISCAP 2013, v. 1, p. 145-151, 2013.

TAUSEL, L. ; CIFUENTES, C. ; RODRIGUEZ, C. ; FRIZERA, A ; BASTOS, TEODIANO FREIRE. Human-Walker Interaction on Slopes Based on LRF and IMU Sensors. In IEEE International Conference on Biomedical Robotics and Biomechatronics - BioRob 2014. In state of revision.

7.4 Future directions

An important future objective is to do tests with the human IMU working so to be able to use the complete version of the control equation used to define the φ angle, explained in equation 4.8.

As future works, it is intended to integrate force sensors, applied to the forearm supports, and other wearable sensors in the Pivot Model in order to strengthen the interpretation of human behavior during walker-assisted gait on slopes. Additionally, the aim is to integrate the model into the control strategies developed for the UFES Smart Walker in

order to actively assist human gait. Meaning with the motors connected to the axis of traction and the walker controlled with the use of the Pivot model control strategy. This set of experiments would be useful to appreciate the correct functioning of the control strategy, both for pitch and roll. For these tests it could be used a U-turn path or a diagonal path.

Furthermore, a clinical validation of the proposed model with locomotion-related pathological subjects is intended to be done in order to better understand the rehabilitative value of the proposed method.

Bibliography

[1] IFR. Service Robots - IFR International Federation of Robotics, 2014. URL http://www.ifr.org/service-robots/.

[2] ISO Robots and robotic devices. ISO 8373:2012(en), 2014. URL https://www.iso.org/obp/ui/#iso:std:iso:8373:ed-2:v1:en.

[3] WORLD ROBOTICS. Executive Summary 2013. Technical report, 2013. URL http://www.worldrobotics.org/uploads/media/Executive_Summary_WR_2013.pdf.

[4] United Nations. Article 21: RIGHT TO HEALTH AND REHABILITATION, 2014. URL http://www.un.org/esa/socdev/enable/rights/ahcwgreporta21.htm.

[5] A. Frizera, R. Ceres, J. L. Pons, and E. Rocon. A platform to study human-machine biomechanical interaction during gait. In *Assistive Technology Research Series - Challenges for Assistive Technology AAATE 07*, number September, 2007.

[6] United Nations. World Population Ageing 2013. Technical report, New York, 2013. URL http://www.un.org/en/development/desa/population/publications/pdf/ageing/WorldPopulationAgeingReport2013.pdf.

[7] A. Frizera and R. Raya. The Smart Walkers as Geriatric Assistive Device. The SIMBIOSIS Purpose. In *International journal on the fundamental aspects of technology to serve the aging society*, pages 212–218, 2008. URL http://www.gerontechnology.info/Journal/Proceedings/ISG08/papers/049.pdf.

[8] C. Vaughan, Brian Davis, and Jeremy O'Connor. *Dynamics of Human Gait*. Kiboho publishers, Cape Town, South Africa, 2 edition, 1999. ISBN 0620235586.

[9] A. Duxbury. Gait disorders and fall risk: Detection and prevention. In *COMP THER*, pages 238–245, 2000.

[10] Maria M. Martins, Cristina P. Santos, Anselmo Frizera-Neto, and Ramón Ceres. Assistive mobility devices focusing on Smart Walkers: Classification and review. *Robotics and Autonomous Systems*, 60(4):548–562, April 2012. ISSN 09218890. doi:

10.1016/j.robot.2011.11.015. URL http://linkinghub.elsevier.com/retrieve/pii/S0921889011002181.

[11] Georgia Institute of technology. Dexterity and Mobility Impairment Fact Shee, 2007. URL http://accessibility.gtri.gatech.edu/assistant/acc_info/factsheet_dexterity_mobility.php.

[12] P. J. Nichols, P. A. Norman, and J. R. Ennis. Wheelchair user's shoulder? Shoulder pain in patients with spinal cord lesions. *Scandinavian Journal of Rehabilitation Medicine*, 11:29–32, 1979.

[13] MN Sawka, RM Glaser, RW Wilde, and TC von Luhrte. Metabolic and circulatory responses to wheelchair and arm crank exercise. *J Appl Physiol Respir Environ Exerc Physiol.*, 49:784–788, 1980. URL http://www.ncbi.nlm.nih.gov/pubmed/6776077.

[14] Nelson Costa and Darwin Caldwell. Control of a biomimetic soft-actuated 10dof lower body exoskeleton. *Proceedings of the First IEEE/RAS-EMBS International Conference on Biomedical Robotics and Biomechatronics*, 2006. URL http://ieeexplore.ieee.org/xpl/login.jsp?tp=&arnumber=1639137&url=.

[15] G. Wasson, J. Gunderson, and S. Graves. Effective shared control in cooperative mobility aids. *Proceedings of the Fourteenth International Florida Artificial Intelligence Research Society Conference*, 1:1–5, 2001.

[16] M. Spenko, H. Yu, and S. Dubowsky. Robotic personal aids for mobility and monitoring for the elderly. *IEEE TRANSACTIONS ON NEURAL SYSTEMS AND REHABILITATION ENGINEERING*, 4(3)::344–351, 2006.

[17] G Lacey and K Dawson-Howe. Evaluation of Robot Mobility Aid for the Elderly Blind. *Proceedings of the Fifth International Symposium on Intelligent Robotic Systems*, 1997.

[18] F. W. van Hook, D. Demonbreun, and B. D. Weiss. Ambulatory devices for chronic gait disorders in the elderly. *AMERICAN FAMILY PHYSICIAN*, 67:1717–1724, 2003.

[19] J. Borenstein, H. R. Everett, L. Feng, and D. Wehe. Mobile robot positioning: Sensors and techniques. *Journal of Robotic Systems*, 14 (4):231–249, April 1997. ISSN 07412223. doi: 10.1002/(SICI)1097. URL http://doi.wiley.com/10.1002/%28SICI%291097-4563%28199704%2914%3A4%3C231%3A%3AAID-ROB2%3E3.3.CO%3B2-1.

[20] P. Trahanias, W. Burgard, A. Argyros, D. Hahnel, H. Baltzakis, P. Pfaff, and C. Stachniss. TOURBOT and WebFAIR: Web-operated mobile robots for tele-presence in populated exhibitions. *IEEE Robotics & Automation Magazine*, pages 77– 89., 2005.

[21] S. MacNamara and G. Lacey. A smart walker for the frail visually impaired. *Proceedings 2000 ICRA. Millennium Conference. IEEE International Conference on Robotics and Automation. Symposia Proceedings (Cat. No.00CH37065)*, 2:1354–1359, 2000. doi: 10.1109/ROBOT.2000.844786. URL http://ieeexplore.ieee.org/lpdocs/epic03/wrapper.htm?arnumber=844786.

[22] Diego Rodriguez-Losada, Fernando Matia, Agustin Jimenez, and Gerard Lacey. Guido, the robotic smartwalker for the frail visually impaired. *First International Conference on Domotics, Robotics and Remote Assitence for All - DRT4all*, 2005. URL http://citeseerx.ist.psu.edu/viewdoc/download?doi=10.1.1.97.5990&rep=rep1&type=pdf.

[23] Y. Hirata, A. Muraki, and K. Kosuge. Motion Control of Passive-Type Intelligent Walker Based on Caster-Like Dynamics. In *9th International Conference on Rehabilitation Robotics, 2005. ICORR 2005.*, pages 477–481. Ieee, 2005. ISBN 0-7803-9003-2. doi: 10.1109/ICORR.2005.1501146. URL http://ieeexplore.ieee.org/lpdocs/epic03/wrapper.htm?arnumber=1501146.

[24] Carlos Cifuentes, Ariel Braidot, Luis Rodríguez, Melisa Frisoli, and Alfonso Santiago. Development of a Wearable ZigBee Sensor System for Upper Limb Rehabilitation Robotics. pages 1989–1994, 2012.

[25] Sehoon Oh, Naoki Hata, and Yoichi Hori. Proposal of Human-friendly Motion Control and its Application to Wheelchair 3 . Analysis of the Phase of a Wheelchair Using a COG Ob- server. In *The 30th Annual Conference of the IEEE Industrial Electronics Society*, pages 436–441, 2004.

[26] Hubert Roth and Jan Chudoba. Mobile Robots for Search and Rescue. In *Proceedings of the 2005 IEEE International Workshop on Safety, Security and Rescue Robotics*, number June, pages 212–217, 2005. ISBN 078038945X. URL http://www2.hawaii.edu/~nreed/ics606/papers/Ruangpayoongsak05ASHKANA01501265.pdf.

[27] Kazuya Yoshida, Keiji Nagatani, Tetsuyoshi Ito, and Hiroaki Kinoshita. Wheels , Tracks and Reciprocal Walking : Challenges to Loose and Steep Slopes. In *ICRA11 Space Robotics Workshop*, pages 1–3, 2011.

[28] Gao Junyao, Gao Xueshan, Zhu Wei, Zhu Jianguo, and Wei Boyu. Coal Mine Detect and Rescue Robot Design and Research. In *2008 IEEE International Conference on Networking, Sensing and Control*, pages 780–785. Ieee, April 2008. ISBN 978-1-4244-1685-1. doi: 10.1109/ICNSC.2008.4525321. URL http://ieeexplore.ieee.org/lpdocs/epic03/wrapper.htm?arnumber=4525321.

[29] Boyu Weijunyao and Gaokejie Lihu. Navigation and Slope Detection System Design for Autonomous Mobile Robot. In *The Ninth International Conference on Electrinic Measurement & Instruments*, pages 654–658, 2009. ISBN 9781424438648.

[30] Cesare Beghi. La normativa sulle Barriere Architettoniche(decreto ministeriale N 236 del 14 giugno 1989). *Adattambiente*, 1:1–18, 2008.

[31] Automobile Club D'Italia. Linee guida per la progettazione degli attraversamenti pedonali, 2011. URL http://www.aci.it/fileadmin/documenti/notizie/Studi_e_ricerche/linee_guida_attraversamenti_pedonali_2011.pdf.

[32] ABNT Associaçao Brasileira de normas Tecnicas. Acessibilidade a edificações, mobiliário,espaços e equipamentos urbanos, ABNT NBR 9050, 2004. URL http://www.aracaju.se.gov.br/userfiles/emurb/2011/07/Normas_NBR9050_AcessibilidadeEdificacoes.pdf.

[33] Chaitanya P. Gharpure and Vladimir a. Kulyukin. Robot-assisted shopping for the blind: issues in spatial cognition and product selection. *Intelligent Service Robotics*, 1(3):237–251, March 2008. ISSN 1861-2776. doi: 10.1007/s11370-008-0020-9. URL http://link.springer.com/10.1007/s11370-008-0020-9.

[34] V. Kulyukin, C. Gharpure, and J. Nicholson. RoboCart: toward robot-assisted navigation of grocery stores by the visually impaired. *2005 IEEE/RSJ International Conference on Intelligent Robots and Systems*, pages 2845–2850, 2005. doi: 10.1109/IROS.2005.1545107. URL http://ieeexplore.ieee.org/lpdocs/epic03/wrapper.htm?arnumber=1545107.

[35] Inc. Adept Techology. 29/10/13 SPH-2200 - Adept Technology, Inc., 2013. URL http://www.adept.com/products/mobile-robots/mobile-transporters/sph-2200/general.

[36] Adept Mobile Robot. PeopleBot, 2011. URL http://www.mobilerobots.com/Libraries/Downloads/PeopleBot-PPLB-RevA.sflb.ashx.

[37] Aarp. Product Report: Eletric Scooter. Technical report, 1995. URL http://www.pridemobility.com/pdf/resourcecenter/articles/scooter/aarp.pdf.

[38] Soon-wook Hwang, Chang-hyuk Lee, and Young-bong Bang. Power-Assisted Wheelchair with Gravity Compensation. *12th International Conference on Control, Automation and Systems*, (Dd):1874–1877, 2012. URL http://ieeexplore.ieee.org/xpl/login.jsp?tp=&arnumber=6393152&url.

[39] Ruoyu Hou, Xiaodong Shi, and Mahesh Krishnamurthy. Design and implementation of a novel power assisted drivetrain for a wheelchair. *2012 IEEE Transportation Electrification Conference and Expo (ITEC)*, pages 1–6, June 2012. doi: 10.1109/ITEC.2012.6243483. URL http://ieeexplore.ieee.org/lpdocs/epic03/wrapper.htm?arnumber=6243483.

[40] Pei Di, Jian Huang, Kosuke Sekiyama, and Toshio Fukuda. Motion control of intelligent cane robot under normal and abnormal walking condition. In *2011 Ro-Man, 20th IEEE International Symposium on Robot and Human Interactive Communication,*, pages 497–502. Ieee, July 2011. ISBN 978-1-4577-1571-6. doi: 10.1109/ROMAN.2011.6005201. URL http://ieeexplore.ieee.org/lpdocs/epic03/wrapper.htm?arnumber=6005201.

[41] Y. Nemoto, S. Egawa, A. Koseki, S. Hattori, T. Ishii, and M. Fujie. Power-assisted walking support system for elderly. In *Proceedings of the 20th Annual International Conference of the IEEE Engineering in Medicine and Biology Society. Vol.20 Biomedical Engineering Towards the Year 2000 and Beyond (Cat. No.98CH36286)*, volume 5, pages 2693–2695. Ieee, 1998. ISBN 0-7803-5164-9. doi: 10.1109/IEMBS.1998.745229. URL http://ieeexplore.ieee.org/lpdocs/epic03/wrapper.htm?arnumber=745229.

[42] Gyung-hwan Yuk, Hong-soo Park, Hong-gul Jun, Byung-ju Dan, and Byeong-rim Jo. Posture balancing control of smart mobile walker for uneven terrain. In *2012 9th International Conference on Ubiquitous Robots and Ambient Intelligence (URAI)*, number 2, pages 63–64. Ieee, November 2012. ISBN 978-1-4673-3112-8. doi: 10.1109/URAI.2012.6462932. URL http://ieeexplore.ieee.org/lpdocs/epic03/wrapper.htm?arnumber=6462932.

[43] Inho Kim, Woonghee Cho, Gyunghwan Yuk, Hyunseok Yang, Byeong-Rim Jo, and Byung-Hoon Min. Kinematic analysis of sit-to-stand assistive device for the elderly and disabled. In *IEEE ... International Conference on Rehabilitation Robotics : [proceedings]*, volume 2011, pages 41–46, January 2011. ISBN 9781424498628. doi: 10.1109/ICORR.2011.5975438. URL http://www.ncbi.nlm.nih.gov/pubmed/22275638.

[44] Toshikatsu Suzuki, Chi Zhu, Masataka Yoshioka, Simazu Shota, Yuichiro Yoshikawa, Yuji Okada, Yuling Yan, Haoyong Yu, and Feng Duan. Power assistance on slope of an omnidirectional hybrid walker and wheelchair. In *2012 IEEE International Conference on Robotics and Biomimetics (ROBIO)*, pages 974–979. Ieee, December 2012. ISBN 978-1-4673-2127-3. doi: 10.1109/ROBIO.2012.6491095. URL http://ieeexplore.ieee.org/lpdocs/epic03/wrapper.htm?arnumber=6491095.

[45] Chun-Hsu Ko, Kuu-Young Young, Yi-Che Huang, and Sunil Kumar Agrawal. Active and Passive Control of Walk-Assist Robot for Outdoor Guidance. *IEEE/ASME Transactions on Mechatronics*, 18(3):1211–1220, June 2013. ISSN 1083-4435. doi: 10.1109/TMECH.2012.2201736. URL http://ieeexplore.ieee.org/lpdocs/epic03/wrapper.htm?arnumber=6215054.

[46] Hyeon-min Shim, Eung-hyuk Lee, Jae-hong Shim, and Sang-moo Lee. Implementation of an Intelligent Walking Assistant Robot for the Elderly in Outdoor Environment. In *9th International Conference on Rehabilitation Robotics, 2005. ICORR 2005.*, pages 452–455. Ieee, 2005. ISBN 0-7803-9003-2. doi: 10.1109/ICORR.2005.1501140. URL http://ieeexplore.ieee.org/lpdocs/epic03/wrapper.htm?arnumber=1501140.

[47] Toshikatsu Suzuki, Chi Zhu, Masataka Yoshioka, Simazu Shota, Yuichiro Yoshikawa, Yuji Okada, Yuling Yan, Haoyong Yu, and Feng Duan. Power assistance on slope of an omnidirectional hybrid walker and wheelchair. *2012 IEEE International Conference on Robotics and Biomimetics (ROBIO)*, pages 974–979, December 2012. doi: 10.1109/ROBIO.2012.6491095. URL http://ieeexplore.ieee.org/lpdocs/epic03/wrapper.htm?arnumber=6491095.

[48] H-k Wu, C-w Chien, Y-c Jheng, C-h Chen, H-r Chen, and C-h Yu. Development of Intelligent Walker with Dynamic Support. pages 5980–5984, 2011.

[49] M Boell Filho and M.C.M. Silva Junior. *Concepção, projeto, dimensionamento e construção de um andador robótico.* PhD thesis, Universidade Federal do Espirito Santo, 2011.

[50] MA Hamzeh, P Bowke, and A Sayegh. The energy costs of ambulation using two types of walking frame. In *Clin Rehabil 2*, pages 1129–1133. Clin Rehabil 2, 1988. URL scholar.google.it/scholar_url?hl=it&q=http://cre.sagepub.com/content/2/2/119.short&sa=X&scisig=AAGBfm2lkoOoUUpJOsVamjDblkgasf53rw&oi=scholarr&ei=rv8yU9HcAYS27Qb1uYG4DQ&ved=0CDUQgAMoAjAA.

[51] Anselmo Neto Frizera. *Interfaz multimodal para modelado, estudio y asistencia a la marcha humana mediante andadores roboticos*. PhD thesis, Universidad de Alcala-Escuela Politecnica Superior, 2010.

[52] Liliane Basso. Palavras e Coisas: Meu colega em uma cadeira de rodas: proposta metodológica para aferir a significação de produtos assistivos por crianças, 2011. URL http://www.simposiodesign.com.br/wp-content/uploads/2011/05/lili_basso.pdf.

[53] Guy Bonsiepe and Yamada Tamiko. *Desenho industrial para pessoas deficientes*. Conselho Nacional de Pesquisas, Brasilia, 2 edition, 1982. URL http://www.worldcat.org/title/desenho-industrial-para-pessoas-deficientes/oclc/312217840.

[54] H Kawata. URG Series Communication Protocol Specification, 2007. URL http://coecsl.ece.illinois.edu/ge423/datasheets/ladar/LaserRangeScannersSCIP20.pdf.

[55] Valmir Schneider. Detecção de pernas utilizando um sensor de varredura laser aplicado a um andador robótico v. In *Anais do XIX Congresso Brasileiro de Automática, CBA 2012.*, pages 1364–1370, 2012. ISBN 9788580010695. URL http://www.eletrica.ufpr.br/anais/cba/2012/Artigos/99181.pdf.

[56] P.S. de Brito Andre and H. Varum. *Accelerometers: principles, structures and applications*. Nova Science Publishers, Inc, 1 edition, 2013. ISBN 978-1-62808-128-2. URL https://www.novapublishers.com/catalog/product_info.php?products_id=42805.

[57] Karandeep Malhi, Subhas Chandra Mukhopadhyay, Julia Schnepper, Mathias Haefke, and Hartmut Ewald. A Zigbee-Based Wearable Physiological Parameters Monitoring System. *IEEE Sensors Journal*, 12(3):423–430, March 2012. ISSN 1530-437X. doi: 10.1109/JSEN.2010.2091719. URL http://ieeexplore.ieee.org/lpdocs/epic03/wrapper.htm?arnumber=5629425.

[58] Advantech. Advantech Enabilng an intelligent Planet, 1983. URL http://www.advantech.com/default.aspx.

[59] Doga. Doga motor and gearmotor, 2014. URL http://www.doga.es/index.php/en/product/d-c-motors/industry.

[60] J Jones. *Mobile Robots: Inspiration to Implementation*. Peters and CRC Press, second edition, 1998. URL http://www.robotbooks.net/mobile-robots-inspiration-to-implementation-flynn-and-jones-11128/.

[61] Carlos Cifuentes. *Human-Robot Interaction based on Wearable IMU Sensor and Laser Range Finder*. PhD thesis, UFES, 2013.

[62] ADEPT. Pioneer 3-AT (P3AT), 2014. URL http://www.mobilerobots.com/researchrobots/p3at.aspx.

[63] C. Rodriguez, C. Cifuentes, L. Tausel, A. Frizera, and T. Bastos. Estimação de velocidade linear em marcha assistida por andador utilizando varredura laser. In *VII Congreso Iberoamericano de Tecnologías de Apoyo a la Discapacidad - IBERDISCAP 2013*, pages 145–151, Vitoria, 2013.

[64] A. Frizera, J. A. Gallego, E. Rocon, J. L. Pons, and R. Ceres. Extraction of user's navigation commands from upper body force interaction in walker assisted gait. *Biomedical engineering online*, 9(1):37, 2010. URL http://www.biomedcentral.com/content/pdf/1475-925X-9-37.pdf.

[65] A. Frizera, A. Elias, J. Del-Ama, R. Ceres, and T. F. Bastos. Characterization of spatio-temporal parameters of human gait assisted by a robotic walker. In *4th IEEE RAS & EMBS International Conference on Biomedical Robotics and Biomechatronics (BioRob)*, pages 1087 – 1091, 2012. doi: 10.1109/BioRob.2012.6290264. URL http://ieeexplore.ieee.org/xpls/abs_all.jsp?arnumber=629026.

[66] CA Vaz and NV Thakor. Adaptive Fourier estimation of time-varying evoked potentials. *IEEE Transactions on Bio-medical Engineering*, pages 448–455, 1989. doi: 10.1109/10.18751. URL http://europepmc.org/abstract/MED/2714824/reload=0;jsessionid=n8sGGGCFQriJsETRUMW8.12.

[67] CA Vaz, X Kong, and N Thakor. An adaptive estimation of periodic signals using a Fourier linear combiner. *Signal Processing, IEEE Transactions on*, 42(1):1–10, 1994. doi: 10.1109/78.258116. URL http://ieeexplore.ieee.org/xpl/login.jsp?tp=&arnumber=258116.

[68] C Riviere. *Adaptive Suppression of Tremor for Improved Human-machine Control*. Phd thesis, Johns Hopkins University, 1995.

[69] Y. Nemoto, S. Egawa, a. Koseki, S. Hattori, T. Ishii, and M. Fujie. Power-assisted walking support system for elderly. *Proceedings of the 20th Annual International Conference of the IEEE Engineering in Medicine and Biology Society. Vol.20 Biomedical Engineering Towards the Year 2000 and Beyond (Cat. No.98CH36286)*, 5(5):2693–2695, 1998. doi: 10.1109/IEMBS.1998.745229. URL http://ieeexplore.ieee.org/lpdocs/epic03/wrapper.htm?arnumber=745229.

[70] G. Wasson, P. Sheth, M. Alwan, K. Granata, and a. Ledoux. User intent in a shared control framework for pedestrian mobility aids. *Proceedings 2003 IEEE/RSJ*

International Conference on Intelligent Robots and Systems (IROS 2003) (Cat. No.03CH37453), 3:2962–2967. doi: 10.1109/IROS.2003.1249321. URL http://ieeexplore.ieee.org/lpdocs/epic03/wrapper.htm?arnumber=1249321.

[71] Kazuma Suzuki and Keitaro Naruse. Robustness of semi-passive dynamic walking models for steep slopes. In *2011 3rd International Conference on Awareness Science and Technology (iCAST)*, pages 303–308. Ieee, September 2011. ISBN 978-1-4577-0888-6. doi: 10.1109/ICAwST.2011.6163160. URL http://ieeexplore.ieee.org/lpdocs/epic03/wrapper.htm?arnumber=6163160.